STRESSES IN A ROTATING TAPERED DISK

WITH NONCENTRAL HOLES

A THESIS

Presented to

The Faculty of the Graduate Division

by

Amrit Kumar Paul

In Partial Fulfillment

of the Requirements for the Degree

Doctor of Philosophy

in the School of Engineering Science and Mechanics

Georgia Institute of Technology

May, 1969

7/25/68

STRESSES IN A ROTATING TAPERED DISK

WITH NONCENTRAL HOLES

Approved:

Date approved by Chairman: *May 27, 1969*

TABLE OF CONTENTS

TABLE OF CONTENTS (Concluded)

LIST OF TABLES

LIST OF ILLUSTRATIONS

NOMENCLATURE AND SYMBOLS

The following terms and symbols have been used in this thesis.

uniform disk   a disk of constant thickness with or without holes

solid disk   a disk with no holes

filled disk   a given disk modified so that all noncentral holes are filled in

conical disk   a linearly tapered disk with knife-edge periphery, taper starting from the axis of the disk

noncentral holes (or eccentric holes)   holes not located at the center of the disk

Whenever simply "tapered disk" is mentioned, it is to be understood that reference is made to the linearly tapered disk. Simple mention of "holes" means circular holes.

a outer radius of the disk

A_1, A_2 constants in the solution of conical disk

A_n, A_n' constants in the infinite series of the stress function $\Phi_{c_1}(r,\theta)$

a_o, a_n Fourier coefficients in cosine series

b radius of the circle on which the centers of the noncentral holes are located

b_n Fourier coefficients in sine series

B_n, B_n' arbitrary constants in the infinite series of the stress function $\Phi_{c_1}(r,\theta)$

c	radius of the noncentral hole
c_o, c_n	Fourier coefficients of a cosine series
C_1, C_2, C_3	arbitrary constants in the stress function $\Phi_o(r)$
C_{1s}, C_{3s}	arbitrary constants in the stress function $\Phi_{c_2}(r,\theta)$
d	inner radius of the disk, i.e. the radius of the central hole
d_n	Fourier coefficients of a sine series
E	Young's modulus
F	$\frac{\gamma}{g} \omega^2 R^2$
f	photoelastic material fringe value
g	acceleration due to gravity
G	shear modulus
h	thickness of the tapered disk at any radius r
k	number of noncentral holes
K	as defined by equation (53) in Saito's solution
M_{1n}, M_{2n}, M_{3n}, M_{4n}	as defined by equations (99, 100, 101, 102)
m	= 0, 1, 2, ..., k-1
n	fringe order in photoelastic analysis, also used as an index of the infinite series
P	= $(1-x)\sigma_{r_o}$
$P_1(x)$, $P_2(x)$	complementary functions of the hypergeometric differential equation
$P_3(x)$	particular integral
p_1, p_2, p_3	radial stress coefficients
q_1, q_2, q_3	tangential stress coefficients
$Q(x)$	= $(1-x)\sigma_{\theta_o}$

R   radius of the tapered disk extended to the knife edge

r   disc radial coordinate

$S_1(x)$ infinite series solution of the hypergeometric differential equation in x

$\overline{S}_1(x)$ logarithmic solution of the same differential equation

$S_2(t)$ infinite series solution of the hypergeometric differential equation in t, where t = 1-x

$\overline{S}_2(t)$ logarithmic solution of the same differential equation

t   = (1-x) in Martin-Bisshopp's solution

t   width of the calibration member in photoelastic analysis

u   radial displacement in the disk

U_0 real part of W_0

U_s real part of W_s

v   tangential displacement in the disk

v   peripheral velocity of the disk in Saito's solution

W_0 complex harmonic function

W_s s^{th} derivative of W_0 defined as $\dfrac{b^s}{(s-1)!} \dfrac{d^s W_0}{db^s}$, where b is the location radius of the noncentral holes

x $= \dfrac{r}{R}$

z   = complex variable = $re^{i\theta}$

λ a nondimensional parameter

γ weight density of the material

ω angular speed in radian per second

θ central angle on the face of the disk, degrees or radians

(ρ, φ) polar coordinates referred to the center of a noncentral hole

$\zeta \qquad = \rho e^{i\varphi}$

$\nu \qquad$ Poisson's ratio

$\Phi_0(r),\ \Phi_{c_1}(r,\theta),\ \Phi_{c_2}(r,\theta)$ stress functions

$\Phi_c(z),\ \psi_c(z),\ \Phi_m(\zeta_m),\ \psi_m(\zeta_m)$ analytic functions in Saito's solution

symmetrical case   defined as the case of rotating disk without noncentral

holes and in which the stresses and strains are functions of

r only

$\epsilon_r \qquad$ radial strain

$\epsilon_{r_0} \qquad$ radial strain in symmetrical case, $\epsilon_{r_0} = \epsilon_{r_0}(r)$

$\epsilon_\theta \qquad$ tangential strain

$\epsilon_{\theta_0} \qquad$ tangential strain in symmetrical case, $\epsilon_{\theta_0} = \epsilon_{\theta_0}(r)$

$\gamma_{r\theta} \qquad$ shear strain

$\sigma_r \qquad$ radial stress

$\sigma_{r_0} \qquad$ radial stress in symmetrical case, $\sigma_{r_0} = \sigma_{r_0}(r)$

$\sigma_\theta \qquad$ tangential stress

$\sigma_{\theta_0} \qquad$ tangential stress in symmetrical case, $\sigma_{\theta_0} = \sigma_{\theta_0}(r)$

$\tau_{r\theta} \qquad$ shear stress

$\Gamma \qquad$ gamma function

Symbols not occurring in this list are defined wherever they are introduced.

SUMMARY

This thesis presents an original method by which the stresses around a noncentral circular hole in a linearly tapered rotating disk containing a central hole and a ring of symmetrically placed noncentral holes can be reliably calculated under the condition of zero traction on the hole boundaries. It also presents an original theoretical analysis for the stress field of a rotating uniform disk with a similar arrangement of holes.

The determination of the stresses tangent to the boundary of a noncentral hole in a linearly tapered rotating disk is accomplished by utilizing, in part, solutions which are either known or available in the literature. The following steps outline the method.

1. First it is imagined that all the noncentral holes in the tapered disk are filled solidly with the disk material. The disk resulting is called a filled disk. Martin-Bisshopp's solution is employed to determine the tangential stresses at points in the filled disk corresponding to points of interest on the hole boundaries in the original disk.

2. Next, the original tapered disk with all of its holes is replaced by an equivalent uniform disk with noncentral holes only. Saito's solution is employed to determine the stresses along the periphery of a noncentral hole of this modified disk. A stress-concentration factor is then defined as the ratio of the hole boundary's tangential stress as determined by Saito's uniform-disk solution to the tangential stress at a corresponding point in the filled uniform disk. Based on this definition,

a set of stress-concentration factors around a noncentral hole is calcu-
lated.

3. Finally, the stress-concentration factors as determined in
step 2 are multiplied with σ_θ stresses in the filled tapered disk obtained
in step 1; this product yields stresses tangent to the boundary of the
noncentral hole in the original tapered disk. It is noted that the posi-
tion of the maximum stress around such boundary depends upon the relative
hole size.

A photoelastic frozen stress analysis is used to verify the stresses
obtained by the method described for three different relative hole sizes.
The stresses obtained from both analyses are found to be in excellent
agreement throughout.

In addition to the above, a theoretical development of a stress
function for a rotating uniform disk with central and noncentral circular
holes is presented. This stress function is constructed by superposing
three particular stress functions. The first of these is related to the
disk with a central hole only and is associated with the body forces due
to centrifugal action; the second introduces periodicity to the stress
field in the disk with a central hole only; and the third introduces ap-
propriate singularities at the centers of the noncentral holes. These
particular functions are each chosen with enough arbitrariness to admit
the introduction of an equilibrating system of stresses along the free
boundaries. The entire analysis pertaining to this is reported in Chap-
ter VIII of the thesis.

CHAPTER I

INTRODUCTION

The present trend toward higher rotation speeds and complex geometry in many types of machinery increases the difficulty of designing various rotating parts of such machines. In particular, rotors subjected to high angular velocities develop in themselves very high stresses which are frequently difficult to analyze. Flywheels, turbine disks, grinding wheels, gears, and rotary valves are just a few examples of such parts.

The stresses in a uniform rotating disk, with or without a central hole, are determined by relatively simple equations (37); but, if the disk is given a taper, the problem is considerably more difficult. When non-central holes are introduced in any rotating disk, even more difficulty is encountered. Holes in rotating disks are frequently desirable, or even required, to accomplish a specific objective such as reduction of weight, axial flow, control of fluids, or dynamic balancing.

The case where a disk has a straight conical taper and also con-tains noncentral holes is especially difficult to analyze. Such a disk design has been used in a modified Tesla turbine (2) as well as numerous other applications.

The present work is concerned with a study of such a problem and presents an original method of predicting the stresses tangent to the boundaries around the noncentral holes in a rotating disk with linear taper. A photoelastic analysis which confirms the results is included.

The method may be extended to any type of tapered disk for which the solution without the noncentral holes is known.

A theoretical analysis of the stress field in a uniform rotating disk with central and noncentral holes is included. Such an analysis, it is believed, has not been developed heretofore. Because of the complicated nature of the resulting equations, no closed form solutions could be reported. Nevertheless, this analysis provides a good beginning for the problem and future investigation along this line is recommended.

CHAPTER II

REVIEW OF LITERATURE

In 1895, Chree (7) first studied the stresses in a rotating
ellipsoid. Included in this classic work is the solution for a flat
disk spinning about its own axis. He demonstrated that the error intro-
duced in the stresses is of the order of five percent when a thin ellip-
soid is substituted for a flat disk having the same overall dimensions.

The most outstanding works of stress analysis in rotating disks
started in 1905 with Stodola (36) and in 1912 with Donath (9). Stodola
included solutions for rotating disks having hyperbolic profiles. His
work and the work of many others are contained in his two classic volumes
"Steam and Gas Turbines." Donath was the first to suggest that an ap-
proximate solution for the conical disk could be obtained by using a
series of flat annular rings each of different thickness approximating
the conical shape. Grammel (12) later (1923) showed that Donath's ap-
proximate solution for conical disk could be extended to disks with arbi-
trary profiles.

Martin (25) in 1923 presented a solution for the conical disk in a
power series obtained from the hypergeometric differential equation in
terms of stress. At the same time, Honegger (16) in Germany solved the
same problem independently in terms of displacement, by using a series
solution. In Martin's solution, numerical evaluation of the stress coef-
ficients corresponding to the values of the argument near which these

series converge slowly or diverge is laborious, and in some cases asymp-
totic approximations are necessary. Bisshopp (6) in 1944 reconsidered
Martin's problem and, by introducing logarithmic solutions, obtained a
set of four series which converge much more rapidly. Bisshopp suggests
approximating a disk of arbitrary profile by means of a series of concen-
tric annular rings, each having conical taper. He provides a table of
stress-coefficients by means of which specific solutions for simple coni-
cal disks are accomplished quite rapidly. Both Martin's and Bisshopp's
solutions are covered in greater detail in Chapter III. Their combined
solution is used as a preliminary step in the development of a solution
for the problem under consideration in this work.

The problems of stresses in thin rotating disks with thickness
variation as a power function of the radius have been discussed by Sen (33),
Kumar and Jogarao (21), and many others. Lee (23) has developed an in-
teresting solution by a stress function method for the case where the
disk has a profile of the form

$$h = c \, \exp(kr^s)$$

where c is the "hypothetic" thickness where kr^s is zero, k and s being
the parametric constants. When k and s have different signs, h decreases
with r and this case is of more practical significance so far as the ro-
tating disk is concerned. On the other hand, the case in which k and s
have the same signs may be found useful in the design of flywheels, since
h then increases with r.

The state of stress in a rotating disk with no plane of symmetry

perpendicular to the axis of rotation has been investigated by Hodge and Papa (15) in 1955. In addition to the usual radial and tangential forces, bending moments were taken into account because of variation in centroidal heights with respect to the radius in the derivation of the equations of motion. The equations of motion are uncoupled, one for centrifugal stresses and the other for the bending moments and were solved by means of a stress function approach. The disk profile was assumed to be a power function of r.

Samanta (32) in 1963 presented a solution to the problem of a non-homogeneous rotating disk in which the modulus of elasticity is considered as

$$E = E_o \, e^{-kr}$$

keeping the thickness of the disk and Poisson's ratio constant. Both the displacement formulation and the stress formulation were employed in con-structing two solutions, and the solutions so obtained were found to check each other.

Sengupta (34), probably, was the first to analyze the stresses in cylindrically aeolotropic rotating disks of hyperbolic and exponential profiles with the following stress-strain relations.

$$\epsilon_r = a_{12}\sigma_\theta + a_{22}\sigma_r$$

$$\epsilon_\theta = a_{11}\sigma_\theta + a_{12}\sigma_r$$

$$\epsilon_z = a_{13}\sigma_\theta + a_{23}\sigma_r$$

$$\gamma_{r\theta} = a_{66}\tau_{r\theta}$$

where a_{11}, a_{12}, . . . etc. are the elastic constants.

A problem of similar nature has been discussed by Bert and Nieden-fuhr (5) who analyzed stretching of a polar-orthotropic disk of varying thickness under arbitrary body forces by a stress function method. The type of orthotropy considered by them is illustrated by the following stress-strain relationships.

$$\epsilon_r = \frac{e\sigma_r - \nu\sigma_\theta}{eE}$$

$$\epsilon_\theta = \frac{\sigma_\theta - \nu\sigma_r}{eE}$$

$$\gamma_{r\theta} = \frac{2c\,\tau_{r\theta}}{eE}$$

where

$$e = \frac{\text{tangential modulus}}{\text{radial modulus}}$$

and

$$c = \frac{eE}{2G}$$

A problem consisting of an annular disk with stiffness varying as a power function of r was solved to illustrate the method.

All of the problems discussed in this chapter down to this point are relatively simple in nature, in view of the fact that they all involve solutions of differential equations in which r is the only independent variable.

In cases where the stress and strain fields depend on both r and θ, and the disk profile varies in some manner other than a power function of r, the mathematical structure of the problem becomes extremely involved. In such cases, either an approximate theoretical solution or an experi-

mental analysis is generally resorted to.

In 1938 Mindlin (26) solved the problem of an eccentrically rotating disk of constant thickness using bipolar coordinates. In 1949 Udoguchi (38) presented a rigorous theoretical analysis of centrifugal stresses in a rotating disk containing an eccentric hole, by use of bipolar coordinates. In 1951 Barnhart, Hale, and Meriam (4) developed an approximate solution for the stresses in a uniform rotating disk with noncentral holes. Their method involved three steps, each fairly simple in itself. These were:

1. solution of stresses in a solid uniform rotating disk;

2. using stress concentration factors for stresses around a circular hole in an infinite plate to modify the stresses determined in step one;

3. a further modification of the stresses to account for the stress gradients was made by using the solution for the stresses around a hole in an infinite plate under pure bending in its plane. A photoelastic frozen stress analysis showed that the stresses obtained experimentally agreed very closely with those obtained through their analysis.

Saito (29,30) made a series of studies concerned with stresses in rotating disks both experimentally and theoretically. In 1954 he presented a theoretical solution for stresses in a uniform rotating disk containing a ring of equi-spaced holes. The disk did not have a central hole and eccentric holes were of the same radii. His solution is based on a complex variable technique in plane elasticity using both polar and rectangular coordinates referred to the center of the disk and to the center of the noncentral holes, respectively. This solution by him is

discussed in detail in the next chapter.

In 1965 Saito and Honma (31) analyzed the stresses in a tapered disk with noncentral holes experimentally by using bonded-wire strain gages. In this case also the disk considered did not have a central hole. No theoretical work was included in this paper.

In 1963 Green, Hooper, and Hetherington (13) presented an interesting numerical solution of the stress distribution in rotating circular disks containing a central hole and a symmetrical array of noncentral holes. Particular attention was given to an annulus with a width of approximately eight hole diameters containing the holes in which the full two dimensional equations were solved. The region outside this annulus was treated as radially symmetric and the stresses there were determined from a simple one dimensional model. Stress distributions were reported for uniform disks of fixed geometry containing 10, 20, and 45 holes.

There have been a number of experimental studies on circular disks containing noncentral holes by the stress freezing technique of photoelasticity. The work of Barnhart, et al. (4) and Newton (28), in this context, are worth mentioning. These investigators mounted their disks on face plates using pins passing through noncentral holes to provide the turning moment. Such a situation is not usually encountered in practice. Armstrong (1) found that rotating a disk in this manner produces a stress pattern somewhat different from that produced when the disk is held and rotated by means of a central shaft. Armstrong, in his analysis of stresses in a rotating, linearly tapered disk with a central hole and containing an array of six noncentral holes, introduced for the first time the phenomenon of "spoke effect," which allows the outer annulus

of the disk to expand somewhat more than would the corresponding portion of a disk having no noncentral holes. He has analyzed the stresses along a radial line passing through one of the noncentral holes for both uniform and tapered disks.

The problem of rotating disks with noncentral holes resembles in many respects the problem of a plate with holes under a biaxial stress field. When a plate is regarded as extended infinitely in all directions, the solution of the stresses around an isolated single hole in it is well known. The presence of other boundaries near the hole usually introduces great mathematical complication. Jeffery (20) using bipolar coordinates obtained the solution of a semi-infinite plate containing two holes of any radii and center distance. The problem of an infinite strip perforated by a circular hole, symmetrically placed between the edges, was solved by Howland (17). An analysis of stresses in a plate containing an infinite row of uniformly spaced holes of equal radii was also obtained by Howland using the complex variable technique. Following the same technique, Ling and Wang (24) solved the problem of a plate under radial tension, perforated by a ring of circular holes.

CHAPTER III

DETAILED DISCUSSION OF THE SOLUTIONS OF MARTIN,
BISSHOPP, AND SAITO

Martin (25) in 1923 developed a theoretical solution for stresses
in rotating disks of conical profile. He formulated the problem in terms
of the radial stress eliminating the tangential stress from the differen-
tial equation of equilibrium with the help of the equation of compati-
bility. The resulting equation was a hypergeometric differential equation
of exponent difference two, which yielded a solution in the form of two
infinite series and a particular integral due to centrifugal body force.
Numerical evaluation of these series at values of the argument near which
they diverge or converge very slowly was found extremely difficult.
Bisshopp (6) in 1944 reconsidered this problem and constructed solutions
by employing linear relations between the hypergeometric functions of
arguments x and (1-x) and two other expansions in terms of the same argu-
ments which involved logarithms.

Saito (30) in 1957 presented a solution for a uniform, rotating
disk without a central hole, but containing a ring of equal sized circular
holes symmetrically placed around the center of the disk. His method of
solution was by means of the complex variable technique in two dimensional
elasticity. He constructed four harmonic functions, two of which were
referred to the polar coordinates (r,θ) at the center of the disk; the
other two were referred to $(\rho,\wp)$ coordinate system at the center of an

arbitrary noncentral hole. The second set of functions was designed to provide singularity at the center of the noncentral holes. The general stress field in the disk was obtained from the combination of these four functions so as to satisfy the appropriate boundary conditions.

The purpose of discussing, in some detail, these solutions in this chapter is to present their results which will help in constructing a theoretical solution for the determination of the stresses around the non-central holes in a linearly tapered disk presented in Chapter IV.

Martin-Bisshopp: Solution of a Conical Disk

The equation of dynamic equilibrium for a conical rotating disk is given by

$$\frac{d}{dr} (hr\ \sigma_{r_0}) - h\sigma_{\theta_0} = -\frac{\gamma}{g}\ h\omega^2 r^2 \tag{1}$$

The equation of compatibility in this case is

$$\epsilon_{r_0} - \epsilon_{\theta_0} = r\ \frac{d\epsilon_{\theta_0}}{dr} \tag{2}$$

which upon rewriting in terms of stress becomes

$$\sigma_{r_0} - \nu\ \sigma_{\theta_0} = \frac{d}{dr} (r\sigma_{\theta_0} - \nu r\ \sigma_{r_0}) \tag{3}$$

The disk thickness is expressed by

$$h = H(1 - \frac{r}{R})$$
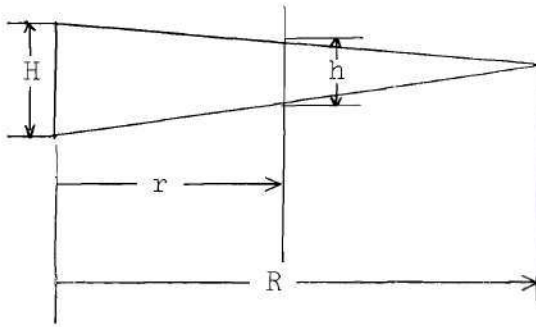
Let $\quad x = \dfrac{r}{R}$

Then $\quad h = H(1-x)$ $\qquad$ (4)

Now, equation (1) in terms of x, and in view of equation (4), becomes

$$\frac{d}{dx}\left[\sigma_{r_0}\, x(1-x)\right] - \sigma_{\theta_0}(1-x) = -\, F\, x^2(1-x) \qquad (5)$$

where

$$F = \frac{\gamma}{g}\,\omega^2 R^2 \qquad (5a)$$

Likewise equation (3) assumes the form

$$(\sigma_{r_0} - \nu\sigma_{\theta_0}) = \frac{d}{dx}(x\sigma_{\theta_0} - \nu x\sigma_{r_0}) \qquad (6)$$

Eliminating σ_{θ_0} from equation (6) with the help of equation (5), the following governing equation results

$$x(1-x)\,\frac{d^2}{dx^2}\,(1-x)\,\sigma_{r_0} + (3-2x)\,\frac{d}{dx}\,(1-x)\,\sigma_{r_0} + (1-\nu)(1-x)\,\sigma_{r_0} \qquad (7)$$

$$= -\,(3+\nu)\, F\, x(1-x)$$

Letting $\qquad\qquad (1-x)\,\sigma_{r_0} = P$

$\qquad\qquad\qquad\qquad\quad (1-x)\,\sigma_{\theta_0} = Q$ $\qquad\qquad$ (8)

one obtains from equation (5)

$$Q = \frac{d}{dx}(Px) + F x^2(1-x) \tag{9}$$

Equation (7), in view of equations (8) and (9), reduces to

$$x(1-x)\frac{d^2P}{dx^2} + (3-2x)\frac{dP}{dx} + (1-\nu)P = -(3+\nu)F x(1-x) \tag{10}$$

the left hand side of which is recognized to be of hypergeometric type, such as

$$x(1-x)\frac{d^2P}{dx^2} + [C - (a+b+1)x]\frac{dP}{dx} - abP = 0 \tag{11}$$

Upon comparing the coefficients of equation (11) with those of equation (10) one finds: $3-2x = c - (a+b+1)x$ and $(1-\nu) = -ab$, i.e., $c = 3$, $(a+b) = 1$, $ab = \nu-1$. Introducing $t = 1-x$ into equation (11) the following hypergeometric equation is obtained.

$$t(1-t)\frac{d^2P}{dt^2} + [a+b+1 - c - (a+b+1)t]\frac{dP}{dt} - abP = 0 \tag{12}$$

The general solution of equation (10) is

$$P(x) = A_1 P_1(x) + A_2 P_2(x) + P_3(x) \tag{13}$$

where $P_1(x)$ and $P_2(x)$ are the complementary functions, and $P_3(x)$ is the particular integral. In fact

$$P_3(x) = \frac{3+\nu}{11+\nu}[x^3 - \frac{7+2\nu}{5+\nu}x^2 - \frac{1-\nu}{5+\nu}x + \frac{3}{5+\nu}] F \qquad (14)$$

The roots of the indicial equation associated with equation (11) are 0 and -2. The integral corresponding to the root 0 is

$$F(a,b,3;x) = S_1(x) = 1 + \frac{a \cdot b}{1 \cdot 3}x + \frac{a(a+1)\,b(b+1)}{1.2.3.4}x^2 + \cdot\cdot\cdot \qquad (15)$$

in which the coefficient of x^n is

$$\frac{a(a+n-1)\,.\,.\,.\,a\,(b+n-1)\,.\,.\,.\,b}{n!\,(n+2)!}$$

The remainder after m terms as given by Bisshopp is

$$R_m < \frac{(m+2)\,x^m\,\sin a\pi}{\pi m^3}$$

which shows that there is a value of $m > N_0$ for $|x| \leqq 1$ which makes the sum of almost all of the terms in the series (15) arbitrarily small, and hence proves the convergence of the series, both absolutely and uniformly. It has been shown in reference (6) that the series derived from equation (15) is also absolutely and uniformly convergent in the interval $|x| \leqq 1$.

Next, the integral belonging to the exponent two is, for convenience, obtained from equation (12) which is equation (11) transformed to use the variable t. Thus

$$t^2 F(a+2,b+2,3,t) = S_2(t) = \frac{2t^2}{ab+2}\left[\frac{ab+2}{2} + \frac{(a+2)(a+1)(b+2)(b+1)}{1!\,3!}t\right.$$

$$\left. + \frac{(a+3)(a+2)(a+1)(b+3)(b+2)(b+1)}{2!\,4!}t^2 + \,.\,.\,.\,.\,.\, \right] \qquad (16)$$

in which the coefficient of t^n (of the terms within the square bracket) is

$$\frac{(n+a+1) \ldots (a+1)(n+b+1) \ldots (b+1)}{n! \, (n+2)!}$$

and the remainder term is (reference 6)

$$R_m < \frac{\sin a\pi}{\pi \, ab(1-t)} \left[m + \frac{t}{1-t} \right] t^m$$

This series evidently diverges when t=1. As would be expected, the difficulties are increased for the derivatives of the infinite series for values of x or t near unity. In view of this, two more series with logarithmic solutions are introduced. These new series converge rapidly when x and t are near zero. As a consequence of the relation 1-x = t, the logarithmic series may be used to construct a convenient form of the function for calculation. Bisshopp has indicated that restricting the values of x and t between 0 and $\frac{1}{2}$ in all four series and their derivatives is sufficient for numerical calculation.

The second solution of equation (11) involves logarithms because the difference of the indicial roots is an integer, the other conditions of the general theory being fulfilled. Thus the logarithmic solution of equation (11) is

$$\overline{S}_1(x) = - \frac{ab(ab+2)}{2} S_1(x) \log_e x + \frac{1}{x^2} - \frac{ab+2}{x} - S_4(x) \tag{17}$$

in which

$$S_4(x) = \sum_{n=2}^{\infty} \frac{(n+a-3)\ \cdots\ (a-2)(n+b-3)\ \cdots\ (b-2)}{n!\ (n-2)!}\ x^{(n-2)}\ \phi_n$$

$$\phi_n = \frac{1}{a-2} + \cdots + \frac{1}{a+n-3} + \frac{1}{b-2} + \cdots + \frac{1}{b+n-3} - 1 - \frac{1}{2}$$

$$- \cdots - \frac{1}{n-2} - 1 - \frac{1}{2} - \cdots - \frac{1}{n}$$

$$\lim_{n\to\infty} \phi_n = \frac{1}{a-2} + \frac{1}{a-1} + \frac{1}{a} - \frac{1}{a+1} - 2\gamma - 2\psi(a) - \pi \cot a\pi$$

$$\gamma = \text{Euler's constant} = 0.577,215,665 \ \cdots$$

$$\psi(a) = \frac{\Gamma'(a+1)}{\Gamma(a+1)} = -\gamma + \lim_{n\to\infty} \sum_{m=1}^{n} \left(\frac{1}{m} - \frac{1}{m+a}\right)$$

where the "prime" indicates differentiation with respect to the argument.

Similarly, the second solution of equation (12), which is a logarithmic solution, is

$$\overline{S}_2(t) = \frac{-a(a+1)\ b(b+1)}{2}\ S_2(t)\ \log_e t + S_3(t) \tag{18}$$

where

$$S_3(t) = 1 - abt - \sum_{n=2}^{\infty} \frac{(n-1+a)\ \cdots\ a(n-1+b)\ \cdots\ b}{n!\ (n-2)!}\ t^n\ \phi_n$$

$$\phi_n = \frac{1}{a} + \cdots + \frac{1}{a+n-1} + \frac{1}{b} + \cdots + \frac{1}{b+n-1} - 1 - \frac{1}{2} - \cdots$$

$$- \frac{1}{n-2} - 1 - \frac{1}{2} \cdots - \frac{1}{n}$$

$$\lim_{n\to\infty} \phi_n = 2\left[\frac{1}{a} - \gamma - \psi(a)\right] - \pi \cot a\pi$$

The details concerning the convergence of the series in equations

(17) and (18) and of the series derived from them are discussed thoroughly in reference (6).

The four solutions, equations (15), (16), (17), and (18) are linearly dependent, since they satisfy two second order differential equations (11) and (12) which are related by the linear transformation, $1-x = t$, in the same interval of convergence $[0,1]$. Therefore, the general solution involving $S_2(t)$ and $\overline{S_2}(t)$ is equivalent to $S_1(x)$ in the interval between zero and unity, i.e.

$$P(t) = C_2 S_2(t) + C_1 \overline{S_2}(t) = S_1(x)$$

where C_1 and C_2 are determined by the following conditions (reference 6)

$$\lim_{t \to 0} P(t) = \lim_{x \to 1} S_1(x) = \frac{2 \sin a\pi}{\pi ab \ (ab+2)} \tag{20}$$

$$\begin{array}{cc} P(t) & = S_1(x) = 1 \\ t \to 1 & x \to 0 \end{array} \tag{21}$$

Equations (19) and (20), in view of the equations (15), (16), and (18) yield

$$C_1 = \frac{2 \sin a\pi}{\pi ab \ (ab+2)} \tag{22}$$

In an analogous manner, it has been shown in reference (6) that

$C_2 = \frac{2 \sin a\pi}{\pi} [\frac{1}{a} - \gamma - \psi(a)] - \cos a\pi$, γ being the Euler's constant.

Equations (13) and (19), together with the relation $1-x = t$ give

$$A_1 P_1(x) = A_1 S_1(x) \tag{23}$$

$$= A_1 \{C_2 S_2(1-x) + C_1 \overline{S}_2(1-x)\} \tag{24}$$

Equation (23) converges very rapidly near x=0, whereas equation (24) does the same near x=1. By using each of these equations in its range of rapid convergence, $P_1(x)$ is computed very easily numerically. The second solution is treated in an analogous manner and is found to be

$$A_2 P_2(x) = A_2 S_2(1-x) \tag{25}$$

$$= A_2 \{C_3 S_1(x) + C_1 \overline{S}_1(x)\} \tag{26}$$

and is very convenient for numerical work, both at x near zero and unity.

The derived series from equations (23), (24), (25), and (26) also exhibit similar behavior of convergence with respect to x near zero and unity.

From the relationship between P and Q defined by equation (9), one obtains

$$\left. \begin{aligned} Q_1 &= \frac{d}{dx}(P_1 x) \\ Q_2 &= \frac{d}{dx}(P_2 x) \\ Q_3 &= \frac{d}{dx}(P_3 x) + F\,x^2(1-x) \end{aligned} \right\} \tag{27}$$

Then the "stress coefficients" as defined by Bisshopp (6) are

$$p_1 = \frac{P_1}{C_1(1-x)} \qquad\qquad q_1 = \frac{Q_1}{C_1(1-x)}$$

$$p_2 = -\frac{P_2}{(1-x)} \qquad\qquad q_2 = -\frac{Q_2}{(1-x)}$$

$$p_3 = \frac{3+\nu}{11+\nu}\left[-x^2 + \frac{2+\nu}{5+\nu}\,x + \frac{3}{5+\nu}\right]$$

$$q_3 = \frac{3+\nu}{11+\nu}\left[-\frac{1+3\nu}{3+\nu}\,x^2 + \frac{1+2\nu}{5+\nu}\,x + \frac{3}{5+\nu}\right]$$

$$(28)$$

These express the stresses σ_{r_0} and σ_{θ_0} in the following form because of equation (13).

$$\sigma_{r_0} = A_1 p_1 + A_2 p_2 + F\,p_3 \qquad\qquad (29)$$

$$\sigma_{\theta_0} = A_1 q_1 + A_2 q_2 + F\,q_3$$

Numerical values of the stress coefficients for a wide range of values of ν are given by Bisshopp corresponding to positive values of x between zero and unity. Table 1, which is reproduced here from reference (6), gives the stress coefficients for $\nu=0.3$ at intervals of $x=0.01$ between zero and unity.

The equations (29) and (30) for a rotating conical disk can be conveniently employed to calculate the centrifugal stresses in any concentric annulus cut from it. In other words, the stresses in a rotating disk with a central hole and a linearly tapered profile can be obtained with the help of these two equations once the constants A_1 and A_2 are evaluated from the known tractions prescribed on the boundaries of the disk.

Table 1. Stress Coefficients in a Conical Disk for $\nu=0.3$

$\frac{r}{R}$	p_1	$-p_2$	p_3	$\frac{r}{R}$	p_1	$-p_2$	p_3
.00	1.433959	∞	.1653031	.50	2.469975	1.743253	.1556604
.01	1.445058	6951.07	.1665412	.51	2.542237	1.647427	.1539781
.02	1.456573	1731.472	.1677209	.52	2.58672	1.557374	.1522375
.03	1.467909	766.511	.1686422	.53	2.63291	1.472654	.1504585
.04	1.479674	429.540	.1679051	.54	2.60105	1.392866	.1485810
.05	1.491675	273.542	.1709096	.55	2.73128	1.317649	.1466651
.06	1.503919	189.0580	.1718957	.56	2.78375	1.246670	.1446909
.07	1.516414	138.2064	.1727434	.57	2.83859	1.179628	.1426682
.08	1.529167	105.2611	.1735726	.58	2.89599	1.116248	.1405671
.09	1.542188	82.7153	.1745435	.59	2.95613	1.056276	.1384176
.10	1.555485	66.6187	.1750559	.60	3.01921	.999482	.1362097
.11	1.569067	54.7317	.1757100	.61	3.00545	.945654	.1339434
.12	1.582943	45.7082	.1763056	.62	3.15511	.894597	.1316187
.13	1.597125	38.6998	.1768429	.63	3.22846	.846132	.1292596
.14	1.611621	33.1500	.1773217	.64	3.30581	.800093	.1267941
.15	1.626444	28.6619	.1777421	.65	3.38749	.756328	.1242941
.16	1.641604	25.0527	.1781041	.66	3.47383	.714697	.1217358
.17	1.657114	22.0147	.1784077	.67	3.56544	.675068	.1191190
.18	1.672986	19.49109	.1786527	.68	3.66261	.637322	.1164439
.19	1.689234	17.36003	.1788397	.69	3.76594	.601347	.1137103
.20	1.705870	15.54461	.1789681	.70	3.87605	.567039	.1109184
.21	1.722911	13.98583	.1790381	.71	3.99364	.534302	.1080680
.22	1.740370	12.63785	.1790497	.72	4.11951	.503046	.1051592
.23	1.758265	11.46457	.1790028	.73	4.25456	.473188	.1021920
.24	1.776612	10.43730	.1788976	.74	4.39987	.444650	.0991664
.25	1.795429	9.53299	.1787339	.75	4.55664	.417360	.0960824
.26	1.814735	8.73295	.1785119	.76	4.72631	.391249	.0929400
.27	1.834550	8.02190	.1782314	.77	4.91057	.366256	.0897392
.28	1.854894	7.38726	.1778925	.78	5.11138	.342321	.0864800
.29	1.875739	6.81856	.1774953	.79	5.33111	.319386	.0831623
.30	1.897260	6.30710	.1770396	.80	5.57258	.297406	.0797863
.31	1.919330	5.84553	.1765255	.81	5.83923	.276326	.0763518
.32	1.942026	5.42766	.1759550	.82	6.13524	.256103	.0728590
.33	1.965375	5.04821	.1753221	.83	6.46578	.236694	.0693077
.34	1.989407	4.70267	.1746328	.84	6.83730	.218058	.0656980
.35	2.01415	4.38719	.1738850	.85	7.25799	.200159	.0620300
.36	2.03965	4.09844	.1730789	.86	7.73837	.182959	.0583035
.37	2.06692	3.83352	.1722144	.87	8.29219	.166279	.0545186
.38	2.09301	3.58693	.1712914	.88	8.93778	.150531	.0506753
.39	2.12097	3.36548	.1703101	.89	9.70015	.135206	.0467736
.40	2.14902	3.15825	.1692703	.90	10.61427	.120527	.0428135
.41	2.17963	2.96657	.1681722	.91	11.73070	.106365	.0387950
.42	2.21043	2.78894	.1670156	.92	13.12522	.092730	.0347180
.43	2.24227	2.62405	.1658006	.93	14.91694	.079556	.0305827
.44	2.27522	2.47075	.1645272	.94	17.30435	.066943	.0263890
.45	2.30933	2.32799	.1631954	.95	20.6447	.054750	.0221368
.46	2.34467	2.19485	.1618052	.96	25.6523	.042950	.0178629
.47	2.38131	2.07051	.1603566	.97	33.9942	.031660	.01345732
.48	2.41931	1.954225	.1588496	.98	50.6706	.020727	.00902995
.49	2.45876	1.845540	.1572822	.99	100.6824	.01017919	.00454418
.50	2.469975	1.743253	.1556604	1.00	∞	0	0

$\frac{r}{R}$	q_1	q_2	q_3	$\frac{r}{R}$	q_1	q_2	q_3
.00	1.433959	∞	.1653031	.50	2.08937	4.94357	.1673485
.01	1.444668	7045.31	.1661679	.51	2.11296	4.00323	.1665319
.02	1.449500	1779.952	.166990	.52	2.13735	4.67024	.1656816
.03	1.457499	799.636	.1677366	.53	2.16259	4.54407	.1647978
.04	1.465548	454.739	.1685605	.54	2.18873	4.42425	.1638902
.05	1.473771	294.278	.1692908	.55	2.21582	4.31032	.1629291
.06	1.482152	206.665	.1699874	.56	2.24391	4.20190	.1619444
.07	1.490634	153.5664	.1706505	.57	2.27308	4.09861	.1609260
.08	1.499282	118.9261	.1712799	.58	2.30339	4.00013	.1598740
.09	1.508080	95.0548	.1718757	.59	2.33491	3.90614	.1587883
.10	1.517031	77.8919	.1724378	.60	2.36773	3.81636	.1576691
.11	1.526142	65.1279	.1729663	.61	2.40195	3.73054	.1565162
.12	1.535415	55.3697	.1734612	.62	2.43765	3.64842	.1553296
.13	1.544857	47.7364	.1739225	.63	2.47495	3.56979	.1541095
.14	1.554473	41.6464	.1743501	.64	2.51396	3.49444	.1528557
.15	1.564267	36.7114	.1747441	.65	2.55483	3.42219	.1515683
.16	1.574246	32.6500	.1751045	.66	2.59771	3.35285	.1502473
.17	1.584415	29.2666	.1754312	.67	2.64275	3.28627	.1488926
.18	1.594780	26.4166	.1757244	.68	2.69014	3.22228	.1475043
.19	1.605348	23.9921	.1759839	.69	2.74010	3.16075	.1460824
.20	1.616125	21.9114	.1762097	.70	2.79285	3.10155	.1446268
.21	1.627119	20.1115	.1764020	.71	2.84866	3.04456	.1431376
.22	1.638336	18.54334	.1765606	.72	2.90783	2.98966	.1416148
.23	1.649785	17.16816	.1766855	.73	2.97071	2.93672	.1400584
.24	1.661473	15.95500	.1767769	.74	3.03769	2.88568	.1384683
.25	1.673408	14.87894	.1768346	.75	3.10923	2.83642	.1368446
.26	1.685601	13.91969	.1768587	.76	3.18584	2.78887	.1351873
.27	1.698059	13.06060	.1768492	.77	3.26815	2.74293	.1334964
.28	1.710793	12.28792	.1768060	.78	3.35686	2.69853	.1317718
.29	1.723813	11.59018	.1767292	.79	3.45284	2.65560	.1300136
.30	1.737130	10.95779	.1766188	.80	3.55710	2.61407	.1282217
.31	1.750754	10.38265	.1764748	.81	3.67035	2.57387	.1263963
.32	1.764699	9.85787	.1762971	.82	3.79558	2.53494	.1245372
.33	1.778977	9.37761	.1760858	.83	3.93510	2.49724	.1226445
.34	1.793601	8.93682	.1758408	.84	4.08565	2.46070	.1207181
.35	1.808585	8.53119	.1755623	.85	4.25607	2.42526	.1187582
.36	1.823945	8.15697	.1752501	.86	4.44796	2.39090	.1167645
.37	1.839696	7.81090	.1749043	.87	4.66601	2.35755	.1147373
.38	1.855855	7.46015	.1745248	.88	4.91641	2.32518	.1126764
.39	1.872439	7.19222	.1741118	.89	5.20754	2.29375	.1105820
.40	1.889468	6.91494	.1736651	.90	5.55103	2.26321	.1084538
.41	1.906962	6.65638	.1731847	.91	5.96355	2.23353	.1062921
.42	1.924942	6.41483	.1726708	.92	6.46909	2.20468	.1040967
.43	1.943431	6.18878	.1721232	.93	7.10866	2.17662	.1018677
.44	1.962453	5.97688	.1715420	.94	7.94365	2.14933	.0996051
.45	1.982034	5.77794	.1709271	.95	9.08864	2.12276	.0973068
.46	2.00820	5.59089	.1702786	.96	10.76913	2.09690	.0949789
.47	2.02209	5.41474	.1695966	.97	13.50620	2.07172	.0926154
.48	2.04442	5.24865	.1688808	.98	18.84745	2.04719	.0902183
.49	2.06653	5.09183	.1681315	.99	34.44457	2.02329	.0877975
.50	2.08937	4.94357	.1673485	1.00	∞	2.00000	.0853231

Saito: Solution of a Uniform Rotating Disk Containing

a Symmetrical Array of Noncentral Holes

The following geometry is used in Saito's solution for a uniform rotating disk without a central hole but containing a symmetrical array of noncentral circular holes.

With reference to Figure 1, (x,y) are the rectangular coordinates referred to the center of the disk as origin; (r,θ) are the corresponding polar coordinates. (Xm, Ym), $(X\acute{m}, Y\acute{m})$ are the rectangular coordinates referred to the mth hole as origin; (ρ_m, φ_m) are the corresponding polar coordinates. (ρ, φ) are the polar coordinates referred to O_0, the center of the "zeroth" noncentral hole, as origin.
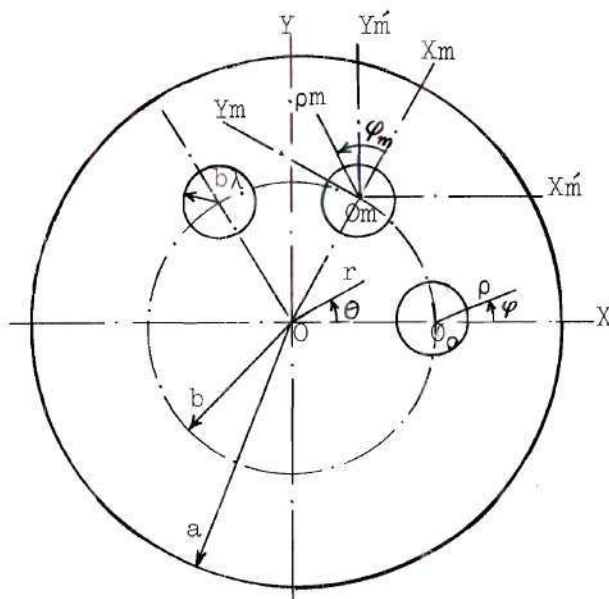

Figure 1.   Coordinate Systems Used in Saito's Solution

The radius of each noncentral hole is taken as $b\lambda$ with the hole centers uniformly spaced around the circumference of a concentric circle of radius b at points represented by

$$z = b\, e^{2im\pi/k} \tag{31}$$

where

k is the number of noncentral holes

and $m = 0,1,2,\ldots,(k-1)$

λ is a dimensionless parameter

$$z = x+iy = are^{i\theta}, \text{ a complex variable} \tag{32}$$

From Figure 1, one can easily see that

$$b\zeta_m = Xm + iYm = b\rho_m\, e^{i\varphi_m} \tag{33}$$

$$b\zeta = z-b = b\rho\, e^{i\varphi} \tag{34}$$

$$\zeta'_m = \zeta_m\, e^{2m\pi i/k} \tag{35}$$

Also using the relation

$$b\zeta'_m = z-b\, e^{2im\pi/k}$$

one obtains from transformation (34)

$$\zeta'_m = 1+\zeta - e^{2im\pi/k} \tag{36}$$

and in view of transformations (35) and (36), ζ_m can be written as

$$\zeta_m = \zeta \, e^{-2im\pi/k} + e^{-2im\pi/k} - 1 \tag{37}$$

Introducing a new variable

$$U_m = \frac{1}{1 - e^{2im\pi/k}} \tag{38}$$

equation (37) is rewritten as

$$\zeta_m = \frac{1 + U_m \zeta}{U_m - 1} \tag{39}$$

On purely physical ground, the following restrictions must hold in order that the boundaries of the holes and of the disk should not overalp.

$$\lambda < \sin\frac{\pi}{k} \quad \text{for} \quad b/a < \frac{1}{1 + \sin\frac{\pi}{k}}$$

$$\lambda < \frac{a}{b} - 1 \quad \text{for} \quad b/a \geqq \frac{1}{1 + \sin\frac{\pi}{k}}$$

As the disk is assumed to be in a state of generalized plane stress, Saito considered the following stress state in the disk with reference to the (x,y) and (r,θ) coordinates.

$$\left.\begin{aligned}
\sigma_x + \sigma_y &= \sigma_r + \sigma_\theta = -\frac{\gamma}{g}\,\omega^2\,\tfrac{1}{2}\,(1+\nu)\,z\bar{z} + 4\,\text{real}\,\Phi_c(z) \\[2mm]
\sigma_y - \sigma_x + 2i\,\tau_{xy} &= (\sigma_\theta - \sigma_r + 2i\,\tau_{r\theta})\,e^{-2i\theta} \\[2mm]
&= \frac{\gamma}{g}\,\omega^2\,\tfrac{1}{4}\,(1-\nu)\,\bar{z}^2 + 2\,[\bar{z}\,\Phi_c'(z) + \psi_c(z)]
\end{aligned}\right\} \tag{40}$$

in which $\Phi_c(z)$ and $\psi_c(z)$ are suitably chosen analytic functions with the property

$$\nabla^2 \; (\Phi_c, \psi_c) = 0 \; , \quad \text{'} \equiv \frac{d}{dz}$$

The stress system referred to the (Xm, Ym) coordinates was taken to be

$$\sigma_x^{(m)} + \sigma_y^{(m)} = 4 \; \text{real} \; \Phi_m \; (\zeta_m)$$

$$\sigma_y^{(m)} - \sigma_x^{(m)} + 2i \; \tau_{xy}^{(m)} = 2 \; [\overline{\zeta}_m \; \Phi_m' \; (\zeta_m) + \psi_m \; (\zeta_m)] \qquad (41)$$

$$\text{'} \equiv \frac{d}{d\zeta_m}$$

with $\quad \nabla^2 \; \Phi_m = 0 \; , \quad \nabla^2 \; \psi_m = 0.$

In view of relations (35) and (36), the stress system in equation (41) was transformed into (r, θ) coordinates as

$$\left. \begin{array}{l} \sigma_r + \sigma_\theta = 4 \; \text{real} \; \Phi_m \left(\frac{z}{b} \, e^{-2im\pi/k} - 1 \right) \\[2ex] \sigma_\theta - \sigma_r + 2i \; \tau_{r\theta} = 2 \; e^{2i(\theta - 2m\pi/k)} \left[\left(\frac{\overline{z}}{b} \, e^{\frac{2im\pi}{k}} - 1 \right) \right. \\[2ex] \left. \Phi_m' \left(\frac{z}{b} \, e^{-2im\pi/k} - 1 \right) + \psi_m \left(\frac{z}{b} \, e^{-2im\pi/k} - 1 \right) \right] \end{array} \right\} \qquad (42)$$

Now, taking the sum of equations (40) and (42), the following stress field for the disk was obtained.

$$\sigma_r + \sigma_\theta = - \frac{\gamma}{g} \, \omega^2 \, \tfrac{1}{2}(1+\nu) \; z\overline{z} + 4 \; \text{real} \left[\Phi_c(z) + \sum_{m=0}^{k-1} \Phi_m \left(\frac{z}{b} \, e^{-2im\pi/k} - 1 \right) \right]$$

(continued)

(equation (43) continued)

$$\sigma_\theta - \sigma_r + 2i\ \tau_{r\theta} = \frac{\gamma}{g}\ \omega^2\ \tfrac{1}{4}\ (1-\nu)\ \bar{z}^2\ e^{2i\theta} + 2\ e^{2i\theta}\ \{\bar{z}\Phi_c'(z) + \psi_c(z)\}$$

$$+ 2\sum_{m=0}^{k-1} e^{2i(\theta - \frac{2m\pi}{k})}\left[\left(\frac{\bar{z}}{b}\ e^{\frac{2im\pi}{K}} - 1\right)\Phi_m'\left(\frac{z}{b}\ e^{-\frac{2im\pi}{k}} - 1\right)\right.$$

$$\left. + \psi_m\left(\frac{z}{b}\ e^{-\frac{2im\pi}{k}} - 1\right)\right]$$

$$\tag{43}$$

Next, using relation (39), the stress system in equation (41) was transformed into (ρ,φ) coordinates as follows

$$\sigma_\rho + \sigma_\varphi = 4\ \text{real}\ \Phi_m\left(\frac{1+U_m\zeta}{U_m-1}\right)$$

$$\sigma_\varphi - \sigma_\rho + 2i\ \tau_{\rho\varphi} = 2\ e^{2i\varphi}\ \frac{U_m^2}{(U_m-1)^2}\left[\frac{1+\bar{U}_m\bar{\zeta}}{\bar{U}_m-1}\ \Phi_m'\left(\frac{1+U_m\zeta}{U_m-1}\right)\right.$$

$$\left. + \psi_m\left(\frac{1+U_m\zeta}{U_m-1}\right)\right]$$

$$\tag{44}$$

And with the help of relations (34), (35), and (37), the stress system in equations (40) was transformed into (ρ,φ) coordinates

$$\sigma_\rho + \sigma_\varphi = -\frac{\gamma}{g}\ v^2\ \tfrac{1}{2}\ (1+\nu)(\tfrac{b}{a})^2\ (1+\zeta+\bar{\zeta}+\zeta\bar{\zeta}) + 4\ \text{Re}\ \Phi_c\ (b+b\zeta)$$

$$\sigma_\varphi - \sigma_\rho + 2i\ \tau_{\rho\varphi} = \frac{\gamma}{g}\ v^2\ \tfrac{1}{4}\ (1-\nu)\ e^{2i\varphi}\ (\tfrac{b}{a})^2\ (1+\bar{\zeta})^2$$

$$+ 2\ e^{2i\varphi}[\,b(1+\bar{\zeta})\ \Phi_c'\ (b+b\zeta) + \psi_c\ (b+b\zeta)]$$

$$\tag{45}$$

where $v = \omega a$ is the peripheral speed of the disk.

The addition of equation (44) to equation (45) led to the following stress system which is referred to (ρ, φ) coordinates for each noncentral hole.

$$
\sigma_\rho + \sigma_\varphi = -\frac{\gamma}{g} v^2 \frac{1}{2}(1+\nu)\left(\frac{b}{a}\right)^2 (1+\zeta+\bar{\zeta}+\zeta\bar{\zeta})
$$

$$
+ 4\,\mathrm{Re}\left[\Phi(\zeta) + \Phi_c(b+b\zeta) + \sum_{m=1}^{k-1}\Phi_m\left(\frac{1+U_m\zeta}{U_m-1}\right)\right]
$$

$$
\sigma_\varphi - \sigma_\rho + 2i\,\tau_{\rho\varphi} = \frac{\gamma}{g}v^2\frac{1}{4}(1-\nu)\,e^{2i\varphi}\left(\frac{b}{a}\right)^2(1+\bar{\zeta})^2
$$

$$
+ 2\,e^{2i\varphi}\left[\bar{\zeta}\,\Phi'(\zeta) + \psi(\zeta) + b(1+\bar{\zeta})\,\Phi_c'(b+b\zeta)\right.
$$

$$
\left. + \psi_c(b+b\zeta)\right] + \sum_{m-1}^{k-1}\frac{U_m^2}{(U_m-1)^2}\left\{\frac{1+\bar{U}_m\bar{\zeta}}{\bar{U}_m-1}\,\Phi_m'\left(\frac{1+U_m\zeta}{U_m-1}\right)\right.
$$

$$
\left. + \psi_m\left(\frac{1+U_m\zeta}{U_m-1}\right)\right\}\Bigg]
$$

$$
\tag{46}
$$

where at m=0 $\Phi_m(\zeta) = \Phi(\zeta)$ and $\psi_m(\zeta) = \psi(\zeta)$.

In view of the fact that the stresses and displacements are single-valued analytic functions in the complete disk and they are repeating with respect to rotation about the origin through angles $\frac{2m\pi}{k}$ and are even with respect to the line of symmetry, Saito assumed the following forms for the harmonic functions

$$
\psi_c(z) = \sum_{s=1}^{\infty} A_s\,(z/a)^{sk-2}
$$

$$
\Phi_c(z) = \sum_{s=0}^{\infty} B_s\,(z/a)^{sk}
$$

$$
\tag{47}
$$

and

$$\psi_m(\zeta) = -K \frac{1}{\zeta_m}(3-\nu) + \sum_{s=2}^{\infty} C_{s-2}\, \zeta_m^{-s}$$

$$\Phi_m(\zeta) = -K \frac{1}{\zeta_m}(1+\nu) + \sum_{s=2}^{\infty} D_{s-2}\, \zeta_m^{-s}$$

(48)

where A's, B's, C's, D's, and K are constant coefficients and remain to
be determined from the boundary conditions.

Now, substituting functions (47) and (48) into the stress equations
(43) and (46) yields the stresses expressed in power series of z and ζ.
Because of the presence of singularities on $r = |z| = b$, the expansion of
equations (43) and (46) into power series is different depending on whether
$|z| < b$ or $> b$.

Saito assumed the boundary tractions in Fourier series.

$$\sigma_r = a_o + \sum_{n=1}^{\infty} a_n \cos nk\theta$$

$$\tau_{r\theta} = \sum_{n=1}^{\infty} b_n \sin nk\theta$$

on $r=1$ (49)

and

$$\sigma_\rho = C_o + \sum_{n=1}^{\infty} C_n \cos n\varphi$$

$$\tau_{\rho\varphi} = \sum_{n=1}^{\infty} d_n \sin n\varphi$$

on $\rho=\lambda$ (50)

and introduced them into the series expansions of equations (43) and (46).

27

Then equating the coefficients of the different powers of z and ζ on both sides of those equations, he obtained the following set of simultaneous equations.

$$2B_0 - k(\frac{b}{a})^2 \, C_0 + 2(1-\nu) \, k(\frac{b}{a})^2 \, K = a_0 + \frac{\gamma}{g} \, v^2 \, \tfrac{1}{8} \, (3+\nu) \; ,$$

$$A_n + (nk-2) \, B_n - \{(1+\nu)(nk+2) \, O_n + p_n\} \, K + \sum_{s=0}^{\infty} {}^n a_s \, C_s$$

$$- \sum_{s=0}^{\infty} \{(nk+2) \, {}^n b_s - {}^n C_s\} \, D_s = -a_n \; , \quad n \geqq 1 \; ,$$

$$A_n + nk \, B_n + \{(1+\nu) \, nk \, O_n + p_n\} \, K - \sum_{s=0}^{\infty} {}^n a_s \, C_s$$

$$+ \sum_{s=0}^{\infty} (nk \, {}^r b_s - {}^n C_s) \, D_s = b_n \; , \quad n \geqq 1 \; ,$$

$$2B_0 - \lambda^{-2} \, C_0 + 2(1+\nu) \, q_0 \, K - \sum_{s=0}^{\infty} {}^o \beta_s \, D_s + \sum_{s=1}^{\infty} {}^o j_s \, B_s$$

$$= C_0 + \frac{\gamma}{g} \, v^2 \, (\frac{b}{a})^2 \, \{\tfrac{1}{4} \, (1+\nu) + \tfrac{1}{8} \, (3+\nu) \, \lambda^2\} \; ,$$

$$-\lambda^{-3} \, C_1 + \{2(3+\nu) \, \lambda^{-1} + q_1 \lambda\} \, K - \lambda \sum_{s=0}^{\infty} {}^1 \beta_s \, D_s + \lambda \sum_{s=1}^{\infty} {}^1 j_s \, B_s$$

$$= c_1 + \frac{\gamma}{g} \, v^2 \, (\frac{b}{a})^2 \, \tfrac{1}{4} \, (3+\nu) \, \lambda \; ,$$

(continued)

(equation (51) continued)

$$-\lambda^{-3} C_1 - \{2(1-\nu)\lambda^{-1} - q_1\lambda\} K - \lambda \sum_{s=0}^{\infty} {}^1\beta_s D_s + \lambda \sum_{s=1}^{\infty} {}^1j_s B_s$$

$$= d_1 - \frac{\gamma}{g} v^2 \left(\frac{b}{a}\right)^2 \frac{1}{4} (1-\nu) \lambda \ ,$$

$$-\lambda^{-4} C_2 + 4\lambda^{-2} D_0 + t_2 K - \sum_{s=1}^{\infty} {}^2\alpha_s C_s + \sum_{s=0}^{\infty} {}^2\gamma_s D_s$$

$$- \sum_{s=0}^{\infty} {}^2f_s A_s - \sum_{s=1}^{\infty} {}^2g_s B_s = C_2 + \frac{\gamma}{g} v^2 \left(\frac{b}{a}\right)^2 \frac{1}{8} (1-\nu),$$

$$-\lambda^{-4} C_2 - 2\lambda^{-2} D_0 + (-2q_2\lambda^2 + t_2) K - \sum_{s=1}^{\infty} {}^2\alpha_s C_s$$

$$+ \sum_{s=0}^{\infty} (2 \ {}^2\beta_s \lambda^2 + {}^2\gamma_s) D_s - \sum_{s=0}^{\infty} {}^2f_s A_s$$

$$- \sum_{s=1}^{\infty} ({}^2g_s + 2 \ {}^2j_s \lambda^2) B_s = -d_2 + \frac{\gamma}{h} v^2 \left(\frac{b}{a}\right)^2 \frac{1}{8} (1-\nu),$$

$$-\lambda^{-n-2} C_n + (n+2) \lambda^{-n} D_{n-2} + \{-(n-2) q_n \lambda^n + t_n \lambda^{n-2}\} K$$

$$- \sum_{s=1}^{\infty} {}^n\alpha_s \lambda^{n-2} C_s + \sum_{s=0}^{\infty} \{(n-2) {}^n\beta_s \lambda^n + {}^n\gamma_s \lambda^{n-2}\} D_s$$

$$- \sum_{s=0}^{\infty} {}^nf_s \lambda^{n-2} A_s - \sum_{s=1}^{\infty} \{{}^ng_s \lambda^{n-2} + (n-2) {}^nj_s \lambda^n\} B_s = C_n,$$

$$n \geq 3,$$

(51)

(equation (51) continued)

$$\lambda^{-n-2} C_n - n \lambda^{-n} D_{n-2} + (-n q_n \lambda^n + t_n \lambda^{n-2}) K$$

$$- \sum_{s=1}^{\infty} {}^n\alpha_s \lambda^{n-2} C_s + \sum_{s=0}^{\infty} (n \, {}^n\beta_s \lambda^n + {}^n\gamma_s \lambda^{n-2}) D_s$$

$$- \sum_{s=0}^{\infty} {}^n f_s \lambda^{n-2} A_s - \sum_{s=1}^{\infty} ({}^n g_s \lambda^{n-2} + n \, {}^n j_s \lambda^n) B_s = -d_n,$$

$$n \geqq 3,$$

where

$${}^n a_s = k\left(\frac{b}{a}\right)^{nk+2} \binom{nk}{s}$$

$${}^n b_s = k\left(\frac{b}{a}\right)^{nk} \binom{nk-1}{s+1}$$

$${}^n c_s = k\left(\frac{b}{a}\right)^{nk+2} (nk+1)\binom{nk}{s+1}$$

$${}^o\beta_s = -2 \sum_{m=1}^{k-1} (U_m - 1)^{s+2}$$

$${}^1\beta_s = (s+2) \sum_{m=1}^{k-1} (U_m - 1)^{s+2} U_m$$

$${}^o j_s = 2\left(\frac{b}{a}\right)^{sk}$$

$${}^1 j_s = sk\left(\frac{b}{a}\right)^{sk}$$

$${}^n\alpha_s = (-1)^n \binom{s+n-1}{s+1} \sum_{m=1}^{k-1} (U_m - 1)^s U_m^n$$

$${}^n\beta_s = (-1)^{n+1} \binom{s+n+1}{s+1} \sum_{m=1}^{k-1} (U_m - 1)^{s+2} U_m^n$$

$$^n\gamma_s = (-1)^{n+1}\,(n-1)\binom{s+n}{s+1}\sum_{m=1}^{n-1}(U_m-1)^{s+1}\,U_m^{n-1}$$

$$^n f_s = \left(\frac{b}{a}\right)^{sk-2}\binom{sk-2}{n-2}$$

$$^n g_s = \left(\frac{b}{a}\right)^{sk}(n-1)\binom{sk}{n-1}$$

$$^n j_s = \left(\frac{b}{a}\right)^{sk}\binom{sk}{n}$$

$$O_n = k\left(\frac{b}{a}\right)^{nk}$$

$$p_n = \left(\frac{b}{a}\right)^{nk+2}k\,\{-nk + 2 - \nu\,(nk+2)\} \tag{52}$$

$$q_n = -\,(1+\nu)\sum_{m=1}^{k-1}(-1)^{n-1}(U_m-1)\,U_m^n$$

$$q_O = \sum_{m=1}^{k-1}(U_m-1)$$

$$t_n = (1+\nu)\sum_{m=1}^{k-1}(-1)^{n-1}(n-1)\,U_m^{n-1} + (3-\nu)\sum_{m=1}^{k-1}\frac{(-1)^{n-2}\,U_m^n}{U_m-1}$$

The solution of equations (51) for the coefficients, namely A_n, B_n, K, etc., yields the following.

$$K = \frac{\gamma}{g}\,v^2\left(\frac{b}{a}\right)\frac{\lambda^2}{8} + \frac{\lambda}{8}\,(a_1-C_1) \tag{53}$$

and

$$B_O = +\,\frac{a_O\lambda^{-2} - k(b/a)^2\,C_O}{2\{\lambda^{-2} - k(b/a)^2\}} + \frac{(\gamma/g)\,v^2}{2\{\lambda^{-2} - k(b/a)^2\}}\left\{\tfrac{1}{8}\,(3+\nu)\,\lambda^{-2}\right.$$

(equation (54) continued)

$$- k \left(\frac{b}{a}\right)^4 \left(\tfrac{1}{4}(1+\nu) + \tfrac{1}{8}(3+\nu)\lambda^2\right)\Big\} - \frac{k(b/a)^2 \, K}{\lambda^{-2} - k(b/a)^2}\Big\{(1-\nu)\lambda^{-2}$$

$$- (1+\nu)q_0\Big\} - \frac{k(b/a)^2}{2\{\lambda^{-2} - k(b/a)^2\}} \sum_{s=0}^{\infty} {}^{o}\beta_s \, D_s + \frac{k(b/a)^2}{2\{\lambda^{-2} - k(b/a)^2\}}$$

$$\times \sum_{s=1}^{\infty} {}^{o}j_s \, B_s ,$$

$$A_n = -\tfrac{1}{2}\{nk\, a_n + (nk-2)\, b_n\} + \{(1+\nu)\, n^2 k^2\, O_n + (nk-1)\, p_n\}\, K$$

$$- \sum_{s=0}^{\infty} (nk-1)\, {}^{n}a_s \, C_s + \sum_{s=0}^{\infty} {}^{n}d_s \, D_s , \qquad n \geq 1 ,$$

$$B_n = \tfrac{1}{2}(a_n + b_n) - \{(1+\nu)(nk+1)\, O_n + p_n\}\, K + \sum_{s=0}^{\infty} {}^{n}a_s \, C_s + \sum_{s=0}^{\infty} {}^{n}e_s \, D_s ,$$

$$n \geq 1$$

$$C_0 = \frac{a_0 - c_0}{\lambda^{-2} - k(b/a)^2} + \frac{(\nu/g)\, v^2}{\lambda^{-2} - k(b/a)^2}\Big\{\tfrac{1}{8}(3+\nu) - \left(\frac{b}{a}\right)^2 \left(\tfrac{1}{4}(1+\nu)\right.$$

$$\left. + \tfrac{1}{8}(3+\nu)\lambda^2\right)\Big\} + \frac{K}{-\lambda^{-2} + k(b/a)^2}\Big\{2(1-\nu)\, k \left(\frac{b}{a}\right)^2 - 2(1-\nu)q_0$$

$$- \frac{1}{\lambda^{-2} - k)b/a)^2} \sum_{s=0}^{\infty} {}^{o}\beta_s \, C_s + \frac{1}{\lambda^{-2} - k(b/a)^2} \sum_{s=1}^{\infty} {}^{o}j_s \, B_s ,$$

$$C_1 = -\tfrac{1}{4}(1-\nu)\, c_1 \lambda^3 - \tfrac{1}{4}(3+\nu)\, d_1 \lambda^3 + q_1 \lambda^4 \, K - \sum_{s=0}^{\infty} {}^{1}\beta_s \, \lambda^4 \, D_s$$

$$+ \sum_{s=0}^{\infty} {}^{1}j_s \, \lambda^4 \, B_s ,$$

(continued)

(equation (54) continued)

$$C_2 = (c_2 - 2d_2)\,\lambda^4 + \frac{\gamma}{g}\,v^2\,\left(\frac{b}{a}\right)^2\,\frac{3}{8}\,(1-\nu)\,\lambda^4 + (4q_2\lambda^6 - 3t_2\lambda^4)\,K \qquad (54)$$

$$+ \sum_{s=0}^{\infty} 3\,^2\alpha_s\,\lambda^4\,C_s - \sum_{s=0}^{\infty} (4\,^2\beta_s\,\lambda^6 + 3\,^2\gamma_s\,\lambda^4)\,D_s$$

$$+ \sum_{s=1}^{\infty} 3\,^2f_s\,\lambda^4\,A_s + \sum_{s=1}^{\infty} (3\,^2g_s\,\lambda^4 + 4\,^2j_s\,\lambda^6)\,B_s,$$

$$D_0 = \frac{1}{2}\,(c_2 - d_2)\,\lambda^2 + \frac{\gamma}{g}\,v^2\,\left(\frac{b}{a}\right)^2\,\frac{1}{8}\,(1-\nu)\,\lambda^2 + (q_2\lambda^4 - t_2\lambda^2)\,K$$

$$+ \sum_{s=0}^{\infty} {}^2\alpha_s\,\lambda^2\,C_s - \sum_{s=0}^{\infty} ({}^2\beta_s\,\lambda^4 + {}^2\gamma_s\,\lambda^2)\,D_s$$

$$+ \sum_{s=1}^{\infty} {}^2f_s\,\lambda^2\,A_s + \sum_{s=1}^{\infty} ({}^2g_s\,\lambda^2 + {}^2j_s\,\lambda^4)\,B_s,$$

$$C_n = \frac{1}{2}\,\{nc_n - (n+2)\,d_n\}\,\lambda^{n+2} + \{n^2 q_n\,\lambda^{2n+2} - (n+1)\,t_n\,\lambda^{2n}\}\,K$$

$$+ \sum_{s=1}^{\infty} (n+1)\,{}^n\alpha_s\,\lambda^{2n}\,C_s - \sum_{s=0}^{\infty} \{n^2\,{}^n\beta_s\,\lambda^{2n+2}$$

$$+ (n+1)\,{}^n\gamma_s\,\lambda^{2n}\}\,D_s + \sum_{s=1}^{\infty} (n+1)\,{}^nf_s\,\lambda^{2n}\,A_s$$

$$+ \sum_{s=1}^{\infty} \{(n+1)\,{}^ng_s\,\lambda^{2n} + n^2\,{}^nj_s\,\lambda^{2n+2}\}\,B_s, \quad n \geqq 3,$$

$$D_{n-2} = \frac{1}{2}\,(c_n - d_n)\,\lambda^n + \{(n-1)\,q_n\lambda^{2n} - t_n\lambda^{2n-2}\}\,K + \sum_{s=0}^{\infty} {}^n\alpha_s\,\lambda^{2n-2}\,C_s$$

$$- \sum_{s=0}^{\infty} \{(n-1)\,{}^n\beta_s\,\lambda^{2n} + {}^n\gamma_s\,\lambda^{2n-2}\}\,D_s + \sum_{s=1}^{\infty} {}^nf_s\,\lambda^{2n-2}\,A_s$$

$$+ \sum_{s=1}^{\infty} \{{}^ng_s\,\lambda^{2n-2} + (n-1)\,{}^nj_s\,\lambda^{2n}\}\,B_s, \quad n \geqq 3$$

where

$$^n d_s = n^2 k^2 \, {}^n b_s - (nk-1) \, {}^n c_s$$

$$^n e_s = - (nk+1) \, {}^n b_s + {}^n c_s$$

(55)

In the case where the disk and the hole have free boundaries

$$a_0 = 0, \quad c_0 = 0, \quad \text{and}$$

$$a_n = b_n = 0$$

$$c_n = d_n = 0$$

for $n \geqq 1$

in equations (53) and (54). K is calculated easily from equation (53). For solving the system of linear equations (54), Saito used the method of perturbation in which λ was considered as the perturbation parameter. It was assumed that the arbitrary constants could be expressed in series of λ as

$$B_0 = \sum_{t=0}^{\infty} B_0^{(2t)} \lambda^{2t+2}$$

$$B_n = \sum_{t=0}^{\infty} B_n^{(2t)} \lambda^{2t+2} \quad , \quad n \geqq 1$$

$$A_n = \sum_{t=0}^{\infty} A_n^{(2t)} \lambda^{2t+2}$$

$$C_0 = \sum_{t=0}^{\infty} C_0^{(2t)} \lambda^{2t+2}$$

$$C_1 = \sum_{t=0}^{\infty} C_1^{(2t)} \lambda^{2t+4}$$

(56)

$$C_2 = \sum_{t=o}^{\infty} C_2^{(2t)} \lambda^{2t+4}$$

$$C_n = \sum_{t=o}^{\infty} C_n^{(2t)} \lambda^{2t+2n+2}, \quad n \geqq 3$$

$$D_0 = \sum_{t=o}^{\infty} D_0^{(2t)} \lambda^{2t+2}$$

$$D_{n-2} = \sum_{t=o}^{\infty} D_{n-2}^{(2t)} \lambda^{2t+2n}, \quad n \geqq 3$$

When equations (56) are substituted into equations (54), the following sets of equations to be solved for the constants are obtained.

$$B_0^{(2t)} = ({}^{t}b_0) + k \left(\frac{b}{a}\right)^2 B_c^{(2t-2)} - \frac{k}{2} \left(\frac{b}{a}\right)^2 {}^{o}\beta_0 D_0^{(2t-2)}$$

$$- \frac{k}{2} \left(\frac{b}{a}\right)^2 \sum_{s=1}^{t-2} {}^{o}\beta_s D_s^{(2t-2s-4)} + \frac{k}{2} \left(\frac{b}{a}\right)^2 \sum_{s=1}^{\infty} {}^{o}j_s B_s^{(2t-2)},$$

$$C_0^{(2t)} = ({}^{t}c_0) + k \left(\frac{b}{a}\right)^2 C_0^{(2t-2)} - {}^{o}\beta_0 D_0^{(2t-2)}$$

$$- \sum_{s=1}^{t-2} {}^{o}\beta_s D_s^{(2t-2s-4)} + \sum_{s=1}^{\infty} {}^{o}j_s B_s^{(2t-2)},$$

$$C_1^{(2t)} = ({}^{t}c_1) - {}^{1}\beta_0 D_0^{(2t-2)} - \sum_{s=1}^{t-2} {}^{1}\beta_s D_s^{(2t-2s-4)}$$

$$+ \sum_{s=1}^{\infty} {}^{1}j_s B_s^{(2t-2)},$$

$$C_2^{(2t)} = ({}^{t}c_2) + 3 \, ({}^{2}\alpha_0 C_0^{(2t-2)} + {}^{2}\alpha_1 C_1^{(2t-4)} + {}^{2}\alpha_2 C_2^{(2t-4)}$$

(continued)

(equation (57) continued)

$$+ \sum_{s=3}^{t-2} {}^2\alpha_s \, C_s \, (2t-2s-2)) - 4 \, {}^2\beta_0 \, D_0 \, (2t-4)$$

$$- 4 \sum_{s=1}^{t-3} {}^2\beta_s \, D_s \, (2t-2s-6) - 3 \, {}^2\gamma_0 \, D_0 \, (2t-2)$$

$$- 3 \sum_{s=1}^{t-2} {}^2\gamma_s \, D_s \, (2t-2s-4) + 3 \sum_{s=1}^{\infty} {}^2f_s \, A_s \, (2t-2)$$

$$+ 3 \sum_{s=1}^{\infty} {}^2g_s \, B_s \, (2t-2) + 4 \sum_{s=1}^{\infty} {}^2j_s \, B_s \, (2t-4) \ ,$$

$$D_0 \, (2t) = ({}^t d_0) + ({}^2\alpha_0 \, C_0 \, (2t-2) + {}^2\alpha_1 \, C_1 \, (2t-4) + {}^2\alpha_2 \, C_2 \, (2t-4)$$

$$+ \sum_{s=3}^{t-1} {}^2\alpha_s \, C_s \, (2t-2s-2)) - {}^2\beta_0 \, D_0 \, (2t-4) - \sum_{s=1}^{t-3} {}^2\beta_s$$

$$\times D_s \, (2t-2s-6) - {}^2\gamma_0 \, D_0 \, (2t-2) - \sum_{s=1}^{t-2} {}^2\gamma_s \, D_s \, (2t-2s-4)$$

$$+ \sum_{s=1}^{\infty} {}^2f_s \, A_s \, (2t-2) + \sum_{s=1}^{\infty} {}^2g_s \, B_s \, (2t-2) + \sum_{s=1}^{\infty} {}^2j_s \, B_s \, (2t-4),$$

$$A_n \, (2t) = ({}^t a_n) - (nk-1)({}^n\alpha_0 \, C_0 \, (2t) + {}^n\alpha_1 \, C_1 \, (2t-2) + {}^n\alpha_2 \, C_2 \, (2t-2)$$

$$+ \sum_{s=3}^{t} {}^n\alpha_s \, C_s \, (2t-2s) + {}^n d_0 \, D_0 \, (2t) + \sum_{s=1}^{t-1} {}^n d_s \, D_s \, (2t-2s-2),$$

$$n \geqq 1 \ ,$$

$$B_n \, (2t) = ({}^t b_n) + ({}^n a_0 \, C_0 \, (2t) + {}^n a_1 \, C_1 \, (2t-2) + \sum_{s=3}^{t} {}^n a_s \, C_s \, (2t-2s))$$

$$+ {}^n e_0 \, D_0 \, (2t) + \sum_{s=1}^{t-1} {}^n e_s \, D_s \, (2t-2s-2), \ n \geqq 1 \ ,$$

(equation (57) continued)

$$C_n^{(2t)} = ({}^tC_n) + (n+1)({}^n\alpha_0\, C_0^{(2t)} + {}^n\alpha_1\, C_1^{(2t-2)}$$

$$+ {}^n\alpha_2\, C_2^{(2t-2)} + \sum_{s=3}^{t} {}^n\alpha_s\, C_s^{(2t-2s)}) - n^2\, {}^n\beta_0\, D_0^{(2t-2)}$$

$$- n^2 \sum_{s=1}^{t-2} {}^n\beta_s\, D_s^{(2t-2s-4)} - (n+1)\, {}^n\gamma_0\, D_0^{(2t)}$$

$$- (n+1) \sum_{s=1}^{t-1} {}^n\gamma_s\, D_s^{(2t-2s-2)} + (n+1) \sum_{s=1}^{\infty} {}^nf_s\, A_s^{(2t)}$$

$$+ (n+1) \sum_{s=1}^{\infty} {}^ng_s\, B_s^{(2t)} + n^2 \sum_{s=1}^{\infty} {}^nj_s\, B_s^{(2t-2)},\ n \geqq 3$$

$$D_{n-2}^{(2t)} = ({}^td_n) + ({}^n\alpha_0\, C_0^{(2t)} + {}^n\alpha_1\, C_1^{(2t-2)} + {}^n\alpha_2\, C_2^{(2t-2)}$$

$$+ \sum_{s=3}^{t} {}^n\alpha_s\, C_s^{(2t-2s)}) - (n-1)\, {}^n\beta_0\, D_0^{(2t-2)}$$

$$- (n-1) \sum_{s=1}^{t-2} {}^n\beta_s\, D_s^{(2t-2s-4)} - {}^n\gamma_0\, D_0^{(2t)}$$

$$- \sum_{s=1}^{t-1} {}^n\gamma_s\, D_s^{(2t-2s-2)} + \sum_{s=1}^{\infty} {}^nf_s\, A_s^{(2t)}$$

$$+ \sum_{s=1}^{\infty} {}^ng_s\, B_s^{(2t)} + (n-1) \sum_{s=1}^{\infty} {}^nj_s\, B_s^{(2t-2)},\ n \geqq 3$$

(57)

where the first terms in the right hand side are determined from the terms containing $\frac{\gamma}{g} v^2$ in equation (54).

It is seen that the validity of the solution by this method depends largely upon the convergence of the series (56). In this context Saito

remarked, "To establish the convergence of such series analytically is very difficult. However, numerical computations carried out for the case when λ is small indicate convergence of these series and seem to give reliable values practically."

In regard to the procedure for determining the constants, one has to adopt the following. First the case of t=0, i.e., the first approximation of the constants has to be determined. Using these values, the second approximation (t=1) can then be found easily from equations (57). In this way, by repeating the calculations, the coefficients of each approximation are determined in terms of the preceding coefficients. After several iterations the coefficients do not change appreciably and the values obtained are taken to be the required ones. In this manner all of the A's, B's, C's, and D's are determined, and hence the functions, equations (47) and (48), are fully known. Upon substitution of these functions into equations (43) and (46), the stresses σ_r, σ_θ, $\tau_{r\theta}$ and σ_ρ, σ_φ, $\tau_{\rho\varphi}$ are completely determined. One of these stresses, namely σ_φ around the edge of the noncentral hole, is extremely important and is readily obtained from the first of equations (46). Noting σ_ρ=0 along the boundary of the hole, one has

$$\sigma_\varphi = \frac{\gamma}{g} v^2 \left(\frac{b}{a}\right)^2 \frac{1}{2} \left[- (1+\nu)(1+\lambda^2) - (1+\nu) \lambda \cos\varphi \right. \tag{58}$$

$$+ \sum_{n=0}^{\infty} q_n \lambda^{n+2} \cos n\varphi] + 4 B_0 + 4 \sum_{n=2}^{\infty} \lambda^{-n} D_{n-2} \cos n\varphi$$

$$+ 4 \sum_{n=0}^{\infty} \left(\sum_{s=1}^{\infty} {}^n j_s B_s - \sum_{s=0}^{\infty} {}^b \beta_s D_s \right) \lambda^n \cos n\varphi$$

This equation is used in Chapter IV in the development of the solution for stresses around noncentral holes in a rotating tapered disk.

CHAPTER IV

DETERMINATION OF STRESS CONCENTRATION FACTORS FOR NONCENTRAL
HOLES IN A ROTATING TAPERED DISK

A determination of stress concentration factors for noncentral
holes in a rotating disk with linear taper is formulated in this chapter
with the help of the results of the analyses presented in Chapter III.
One has already seen that the solution of Martin and Bisshopp presents
an analytical method of determining the centrifugal stresses in tapered
disk with a central bore, whereas the solution of Saito determines the
stresses in a rotating uniform disk containing a symmetrical set of non-
central holes only. By suitably combining these two theories, an analy-
tical method is developed here for the determination of the stress con-
centration factors and hence the stresses along the boundary of a noncentral
hole.

The method so developed is limited to relatively small angles of
taper, that is, for which a plane-stress solution is valid. In addition,
it is further postulated that the stress concentration factors for a hole
in the centrifugal field of a uniform disk will apply to a geometrically
similar hole similarly situated in the centrifugal field of a tapered disk
having the same outside diameter as that of the uniform one.

As was shown, the tangential stress, σ_φ, at the edge of the non-
central hole in a uniform rotating disk is given by (Eq. 58, Chapter III)

$$\sigma_\varphi = \frac{\gamma}{g} \, v^2 \, \left(\frac{b}{a}\right)^2 \, \tfrac{1}{2} \, \{ - \, (1+\nu)(1+\lambda^2) \, - \, (1+\nu) \, \lambda \, \cos\varphi \tag{58}$$

$$+ \sum_{n=0}^{\infty} q_n \, \lambda^{n+2} \, \cos n\varphi \} + 4 \, B_0 + 4 \sum_{n=2}^{\infty} \lambda^{-n} \, D_{n-2} \, \cos n\varphi$$

$$+ 4 \sum_{n=0}^{\infty} \left(\sum_{s=1}^{\infty} {}^n j_s \, B_s \, - \, \sum_{s=0}^{\infty} {}^n \beta_s \, D_s \right) \lambda^n \, \cos n\varphi$$

in which the constant coefficients B's and D's contain the term $\frac{\gamma}{g} \, v^2$ in them. Saito defined a stress concentration factor based on the maximum stress in the corresponding solid disk in the following manner. The maximum stress in a rotating uniform solid disk occurs at its center and it is (Ref. 37, p. 71)

$$\sigma_0 = \frac{3+\nu}{8} \cdot \frac{\gamma}{g} \, v^2 \, , \quad \text{where} \quad v^2 = (\omega a)^2 \tag{59}$$

Let σ_φ, equation (58), be divided by σ_0, equation (59) and call the quotient k_s (Saito's stress concentration factor). k_s may be then expressed in this form.

$$k_s = A + B \cos\varphi + C \cos 2\varphi + D \cos 3\varphi + \, . \, . \, . \tag{60}$$

where

$$A = \frac{8g}{(3+\nu) \, \gamma v^2} \left[- \, \tfrac{1}{2} \, \frac{\gamma}{g} \, v^2 \, \left(\frac{b}{a}\right)^2 \, \{ (1+\nu)(1+\lambda^2) \, - \, q_0 \lambda^2 \} + 4 \, B_0 \right.$$

$$\left. + 4 \left(\sum_{s=1}^{\infty} {}^o j_s \, B_s \, - \, \sum_{s=0}^{\infty} {}^o \beta_s \, D_s \right) \right]$$

$$B = \frac{8g}{(3+\nu)\,\gamma v^2}\left[-\tfrac{1}{2}\frac{\gamma}{g}v^2\left(\frac{b}{a}\right)^2(1+\nu)\lambda + \tfrac{1}{2}\frac{\gamma}{g}v^2\left(\frac{b}{a}\right)^2 q_1\lambda^3\right.$$

$$\left. + 4\left(\sum_{s=1}^{\infty}{}^1\!j_s\,B_s - \sum_{s=0}^{\infty}{}^1\!\beta_s\,D_s\right)\lambda\right]$$

$$C = \frac{8g}{(3+\nu)\,\gamma v^2}\left[\tfrac{1}{2}\frac{\gamma}{g}v^2\left(\frac{b}{a}\right)^2 q_2\lambda^4 + 4\,\lambda^{-2}\,D_0 + 4\left(\sum_{s=1}^{\infty}{}^2\!j_s\,B_s\right.\right.$$

$$\left.\left. - \sum_{s=0}^{\infty}{}^2\!\beta_s\,D_s\right)\lambda^2\right]$$

$$D = \frac{8g}{(3+\nu)\,\gamma v^2}\left[\tfrac{1}{2}\frac{\gamma}{g}v^2\left(\frac{b}{a}\right)^2 q_3\lambda^5 + 4\,\lambda^{-3}D_1 + 4\left(\sum_{s=1}^{\infty}{}^3\!j_s\,B_s\right.\right.$$

$$\left.\left. - \sum_{s=0}^{\infty}{}^3\!\beta_s\,D_s\right)\lambda^3\right] \qquad \text{etc.}$$

The values of A, B, C, D, etc. are obviously dependent on B's, D's, q_n, ${}^n\!j_s$, ${}^n\!\beta_s$, etc. which in turn are determined from equations (52) and (56) in Chapter III. Saito has reported these values in his paper (Ref. 30) for several values of $\frac{b}{a}$, λ, k, and ν. Table 2 shows one such set of values for k = 6 and ν = 0.3.

For the present problem of determining stresses around the non-central holes in a tapered disk, these results are very conveniently employed as follows.

We define the stress concentration factor at a point on the boundary of a noncentral hole in a uniform rotating disk as the ratio of the stress tangent to the boundary at the point of interest to the tangential stress that would occur at the same point in a corresponding uniform solid disk. This enables one to see the influence of the noncentral hole on the

Table 2. Values of A, B, C, D, etc. in equation (60) for k = 6 and ν = 0.3

b/a	λ	A	B	C	D	E	F	G	H
3/5	0	1.433	0	0.305	0	0	0	0	0
	0.10	1.436	-0.056	0.276	0.016	-0.001	-0.000	0.000	-0.000
	0.15	1.441	-0.082	0.244	0.050	-0.004	-0.001	0.000	-0.000
	0.156	1.442	-0.084	0.240	0.057	-0.005	-0.001	0.000	-0.000
	0.20	1.450	-0.106	0.206	0.110	-0.013	-0.005	0.002	-0.000
	0.243	1.462	-0.123	.175	0.190	-0.027	-0.010	0.006	-0.000
	0.25	1.464	-0.126	0.170	0.204	-0.030	-0.012	0.007	-0.001
	0.30	1.495	-0.144	0.136	0.339	-0.052	-0.024	0.015	-0.001
3/7	0	1.711	0	0.156	0	0	0	0	0
	0.10	1.717	-0.028	0.132	0.015	-0.001	-0.000	0.000	-0.000
	0.15	1.726	-0.042	0.106	0.049	-0.005	-0.001	0.000	-0.000
	0.20	1.740	-0.053	0.077	0.112	-0.017	-0.005	0.002	-0.000
	0.25	1.762	-0.064	0.047	0.205	-0.039	-0.012	0.007	-0.001
	0.30	1.798	-0.074	0.020	0.335	-0.077	-0.025	0.016	-0.001
3/10	0	1.858	0	0.076	0	0	0	0	0
	0.10	1.863	-0.014	0.057	0.015	-0.001	-0.000	0.000	-0.000
	0.15	1.869	-0.021	0.036	0.049	-0.006	-0.001	0.000	-0.000
	0.20	1.879	-0.026	0.012	0.110	-0.018	-0.004	0.002	-0.000
	0.25	1.897	-0.031	0.015	0.208	-0.043	-0.011	0.009	-0.001
	0.30	1.922	-0.037	0.042	0.337	-0.083	-0.021	0.017	-0.003

magnitude of the stress that would exist in a corresponding unperforated disk. Thus the stress concentrations around the noncentral hole based on this principle is

$$k_1 = \frac{\sigma_\varphi}{(\sigma_{\theta_o})_u} \tag{61}$$

where $(\sigma_{\theta_o})_u$ = tangential stress in solid, uniform rotating disk at a point corresponding to the location where σ_φ is the stress tangent to the boundary of a noncentral hole in a uniform perforated disk of otherwise similar geometry

By (Ref. 31, p. 71)

$$(\sigma_{\theta_o})_u = \frac{3+\nu}{8} \frac{\gamma}{g} \omega^2 a^2 \left(1 - \frac{1+3\nu}{3+\nu} \frac{r^2}{a^2}\right) \tag{62}$$

Using k_s from equation (60), equation (61) is rewritten as

$$k_1 = k_s \frac{\sigma_o}{(\sigma_{\theta_o})_u} \tag{63}$$

In view of equations (59), (60), and (62), equation (63) becomes

$$k_1 = (A + B \cos\varphi + C \cos 2\varphi + \ldots) \frac{1}{\left(1 - \frac{1+3\nu}{3+\nu} \frac{r^2}{a^2}\right)} \tag{64}$$

This result will now be applied to the tapered disk in determining its stresses around the noncentral holes. Initially the disk of interest is imagined to be replaced by a "filled" disk. That is, a disk geometrically similar except that all noncentral holes are filled with disk material.

Any central hole is undisturbed. Then by following the procedure due to Martin and Bisshopp, the tangential stress in this disk is calculated using equation (30) in Chapter III. The constants A_1, A_2 appearing in this equation are evaluated from the known boundary tractions prescribed on the outer and inner edges of the disk. Next, to determine the actual stress at a point on the boundary of a noncentral hole in this tapered disk, the factor k_1, equation (64), is used to multiply the stress at a corresponding point as obtained from Martin-Bisshopp's solution. Thus

$$\sigma_{\varphi \text{ tapered}} = k_1 \; \sigma_{\theta_0 \text{ tapered}} \tag{65}$$

where $\sigma_{\theta_0 \text{ tapered}}$ is the tangential stress at the point of interest in a corresponding tapered disk without the eccentric holes and is given by equation (30), Chapter III

$$\sigma_{\theta_0 \text{ tapered}} = A_1 q_1 + A_2 q_2 + F q_3 \tag{30}$$

where F, q_1, and q_2 have their meanings defined by equations (5a) and (28) in Chapter III. Further, q_1, q_2, and q_3 are obtained from Table 1.

Introducing equations (64) and (30) into equation (65) one obtains

$$\sigma_{\varphi \text{ tapered}} = (A + B \cos\varphi + C \cos 2\varphi + \ldots) \frac{A_1 q_1 + A_2 q_2 + F q_3}{\left(1 - \frac{1+3\nu}{3+\nu} \frac{r^2}{a^2}\right)} \tag{66}$$

From equation (64) it is obvious that k_1 is a function of (r, φ, ν). For geometrically similar disks, if Poisson's ratio is the same, this fac-

tor k_1 itself is independent of speed and mass density.

The concentration factor k_s is based on the stress at the center of a uniform rotating disk without a central hole. The factor was then redefined as k_1 which is based on a local stress rather than a central stress, but still referred to a solid uniform disk. The justification for the application of k_1 to a tapered disk with a central hole lies in an assumption that the local stress concentration will behave in the same manner if the noncentral holes for the two cases have the same diameters and location radii. In this way, if the actual disk contains a central hole, the filled disk will also contain a central hole, and the effect of such a central hole is thus included in the analysis.

A better result would undoubtedly be obtained if k_1 is based on a uniform rotating disk with a central hole and containing a ring of periodic noncentral holes. An analysis for such a problem is difficult because of the algebra involved (see Chapter VIII).

As an illustration of the application of the theory developed here, consider a tapered disk of plastic having mass density 1.152×10^{-4} lb-sec^2 per in.^{4}. The pertinent dimensions of the disk are given in Figure 2. The speed of rotation is 1680 r.p.m.

The initial step is to obtain the solution for a similar disk, but without the noncentral holes, that is, a filled disk. In view of this, it is necessary to determine first the constants A_1 and A_2 in equation (66) using the proper boundary conditions in Martin-Bisshopp's solution, equation (29), Chapter III.

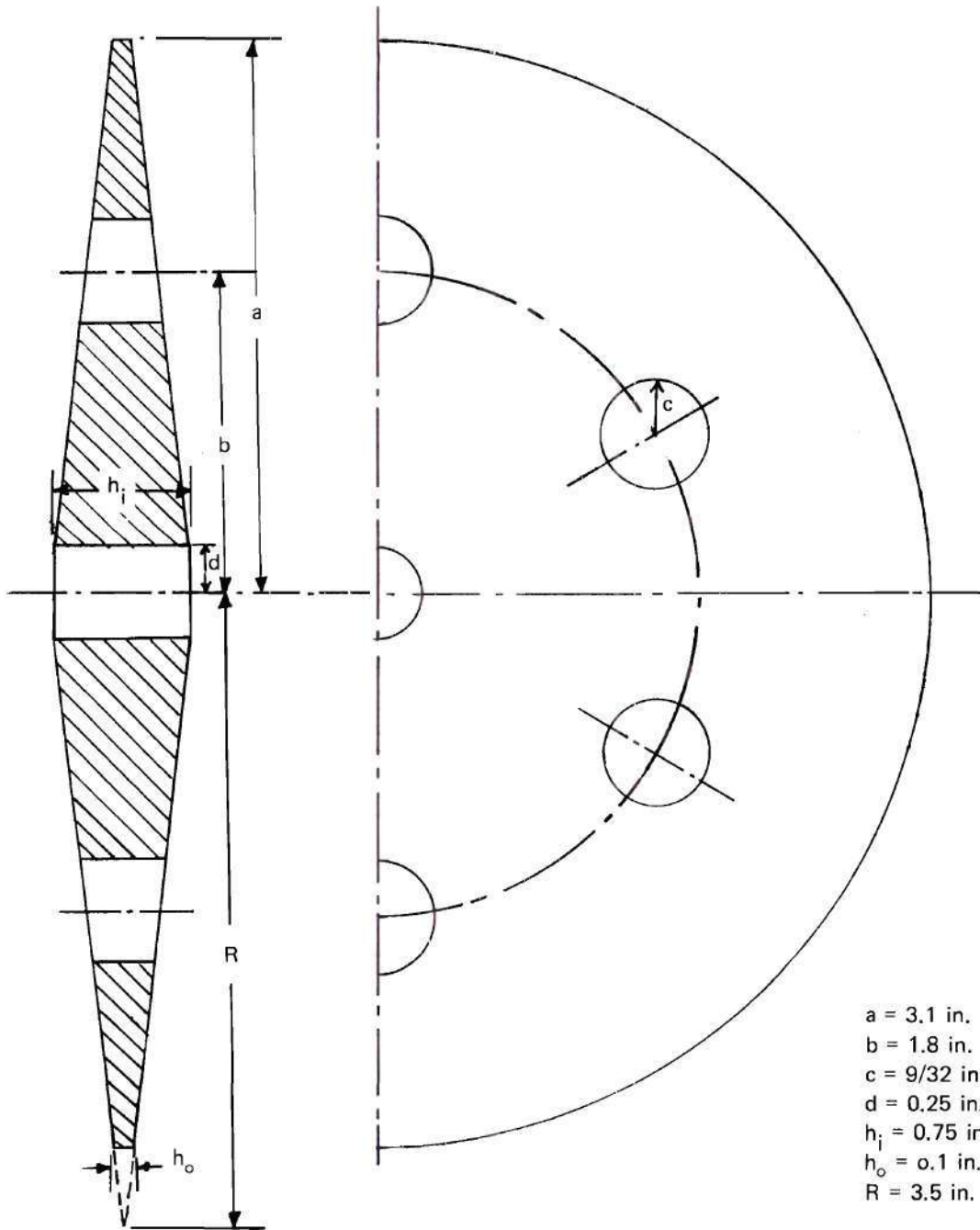For the disk under consideration

47

a = 3.1 in.
b = 1.8 in.
c = 9/32 in.
d = 0.25 in.
h_i = 0.75 in.
h_o = o.1 in.
R = 3.5 in.

Figure 2.   Profile of a Tapered Disk Containing Six 9/16 Inch
           Diameter Noncentral Holes

inside radius   d = 0.25 inch

outside radius a = 3.10 inches

radius up to the knife edge, R = 3.50 inches

Since   x = r/R

One obtains for the inner edge

$$x_i = \frac{d}{R} = \frac{0.25}{3.50} = 0.0715$$

and for the outer edge

$$x_o = \frac{a}{R} = \frac{3.10}{3.50} = 0.885$$

Angular speed of the disk

$$\omega = \frac{2\pi(1680)}{60} = 175.8 \text{ rad./sec}$$

$$F = \frac{\gamma}{g}\,\omega^2 R^2$$

$$= (1.152 \times 10^{-4})(175.8)^2(3.500)^2$$

$$= 43.7 \text{ psi}$$

Corresponding to the values of x_i, x_o the stress coefficients p_1, p_2, p_3 in equation (29) are obtained from Table 1 in Chapter III. The inner and outer boundaries of the disk are free from tractions and hence

$$\left(A_1 p_1 + A_2 p_2 + F p_3\right)_{r=d} = \sigma_{r_o}\Big|_{r=d} = 0$$

$$(A_1 p_1 + A_2 p_2 + F p_3)_{r=a} = \sigma_{r_0}\Big|_{r=a} = 0$$

Substituting the values of p_1, p_2, p_3 from the table into these equations, one obtains

$$A_1\,(1.5183) + A_2\,(-133.2647) + (43.750)(0.1728) = 0$$

$$A_1\,(9.3188) + A_2\,(-0.1428) + (43.750)(0.0487) = 0$$

The solution of these equations yields

$$A_1 = -0.2305$$

$$A_2 = 0.0542$$

Now, using equation (66), which was derived from the stress concentration factors as described earlier in this chapter, the boundary stresses around a noncentral hole will be found. Thus for $\varphi = 0°$ (see Figure 2)

$$r = 2.081 \text{ inches}$$

$$x = \frac{2.081}{3.500} = 0.595$$

and from Table 1 corresponding to this x

$$q_1 = 2.3518$$

$$q_2 = 3.8612$$

$$q_3 = 0.1582$$

For the type of material considered here, ν is taken as 0.3. Substituting these values and the values of A, B, C, etc. from Table 2 corresponding to

λ (i.e. ratio of the radius of the noncentral hole to the location radius of holes) = 0.156 into equation (66), one obtains

$$\sigma_\varphi = \frac{[1.442 - 0.084(1) + 0.24(1) + 0.057(1) - 0.005(1) - 0.001(1) + 0 - 0] \times [-0.2322 \ (2.3672) + 0.053 \ (3.9138) + 43.750 \ (0.1572)]}{1 - \frac{1.900}{3.300} \left(\frac{2.081}{3.100}\right)^2}$$

$$= \frac{(1.649)(6.5865)}{0.7380}$$

$$= 14.700 \text{ psi}$$

The stresses around the noncentral hole for other values of φ are calculated in a similar way and displayed in Table 3. Only the stresses on one half of the circumference are shown, as the other half is symmetrical.

Table 3. Theoretical Stresses Around 9/16 Inch Diameter Noncentral Holes in the Tapered Disk Shown in Figure 2

| φ deg.	σ_φ psi
0	14.700
30	13.380
60	10.725
90	10.800
120	12.400
150	14.000
180	14.850

In addition to this disk, the stresses around the noncentral holes

in two other disks, whose dimensions and profiles are shown in Figure 3, were also calculated. The disk which contains three-fourths inch diameter noncentral holes had a speed of rotation of 2670 rpm and the other disk with seven-eighths inch diameter holes had a speed of rotation of 1680 rpm. The stresses resulting from such calculations are given in Tables 4 and 5.

Table 4. Theoretical Stresses Around 3/4 Inch Diameter Noncentral Holes, rpm 2670

φ deg.	σ_φ psi
0	37.200
30	33.100
60	26.600
90	27.200
120	32.040
150	35.400
180	35.600

$A_1 = -0.604$, $A_2 = 0.130$, $F = 110.400$ psi, $\lambda = 0.208$

$h_o = 0.125''$

$R = 3.75''$

$a = 3.1''$

$b = 1.8''$

$d = 0.25''$

$h_i = 0.6''$
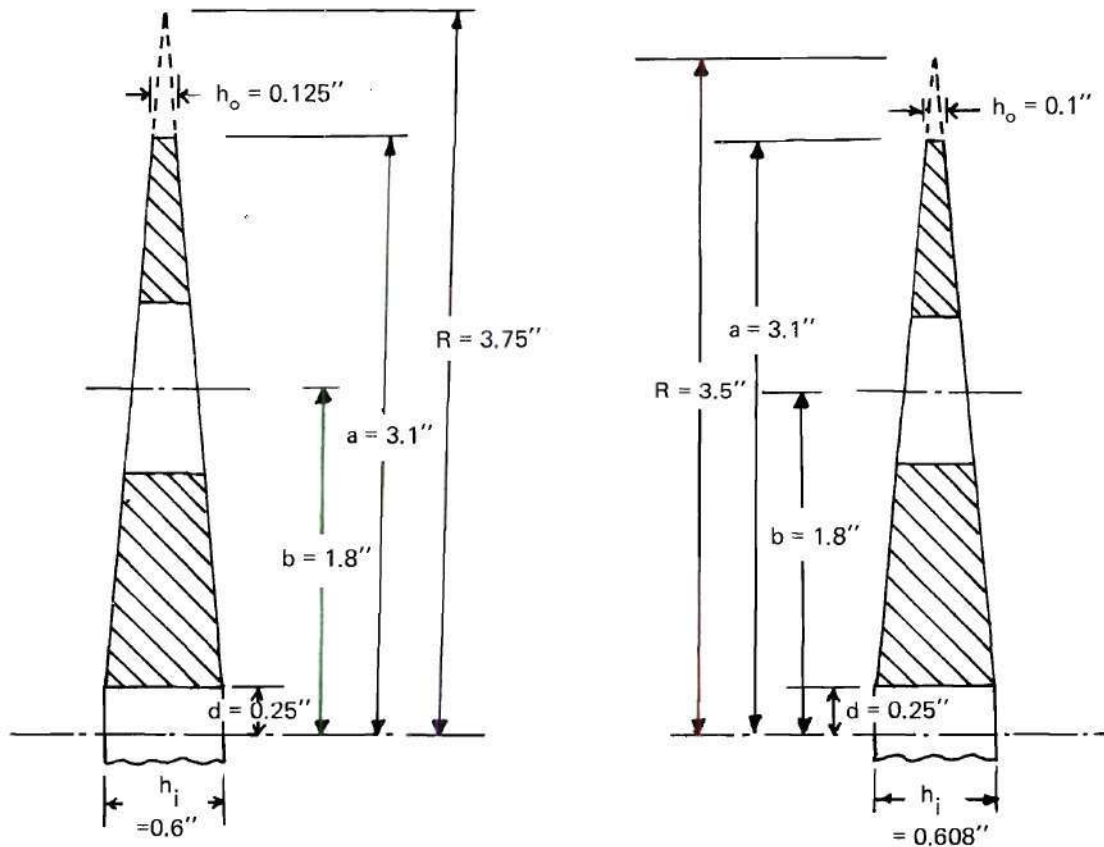
a. PROFILE OF A DISK CONTAINING 7/8 INCH. DIAM. NONCENTRAL HOLES.

$h_o = 0.1''$

$a = 3.1''$

$R = 3.5''$

$b = 1.8''$

$d = 0.25''$

$h_i = 0.608''$

b. PROFILE OF A DISK CONTAINING 3/4 INCH. DIAM. NONCENTRAL HOLES.

Figure 3. Tapered Disk Profiles

Table 5. Theoretical Stresses Around 7/8 Inch Diameter
          Noncentral Holes, rpm 1680

φ deg.	σ_φ psi
0	16.400
30	14.550
60	11.000
90	11.900
120	15.556
135	16.000
150	15.330
180	14.400

$A_1 = -0.555$, $A_2 = 0.0492$, $F = 50.400$ psi, $\lambda = 0.243$

In Chapter V the results given in Tables 3, 4, and 5 are verified
photoelastically.

CHAPTER V

PHOTOELASTIC ANALYSIS OF STRESSES AROUND NONCENTRAL

HOLES IN A ROTATING TAPERED DISK

In order to verify the results of the theoretical solution presented
in the previous chapter, an experimental procedure was needed. Photoelas-
tic stress analysis was considered the best for the purpose. In this
chapter, a photoelastic analysis of the stress field around the noncentral
holes in the tapered disk is described and compared with the results theo-
retically obtained. The procedure adopted here is the well known "frozen
stress" technique in standard photoelastic analysis.

Experimental Procedure

Models

For photoelastic analysis, three disk models and a calibration
member of Bakelite ERL 2795 epoxy resin cured with ZZ-L-0814 were cast in
aluminum moulds using ordinary paste wax as a mould release. The mixture
ratio of 40 parts by weight of ZZ-L-0814 to 100 parts of ERL 2795 was
used. This mixture ratio has been used by other investigators at Georgia
Tech and has proved very satisfactory. It should be mentioned that the
curing reaction for larger quantities of this plastic becomes highly exo-
thermic 10 to 15 minutes after the initial mixing, and it was necessary
to pre-chill the molds for the disks with ice water and to keep them cool
for the first half hour or so. The small mold for the calibration member

did not require cooling due to its smaller mass but, in fact, was heated slightly by means of a light bulb hung over it in order that its curing time and temperature would approximate those of the disks. After removal from the molds, in order to insure more uniform curing, the castings were put in the stress freezing oven and given a post-cure which consisted of the following cycle.

1. Heating to 250°F, 30 minutes, manual control.

2. Soaking at 250°F, 120 minutes, automatic control.

3. Cooling to room temperature, 5°F per hour, automatic control.

Each disk was machined on a Bridgeport milling machine, the indexing head of which was used to mount the disk during machining. The holes were first drilled slightly under size and then brought to size by milling and reaming. The taper was cut by means of an end mill, swiveling the index head an appropriate amount and then rotating the head with the disk mounted on it. The calibration member was machined on a Gorton Pantograph router; a Palmgreen adjustable rotating head was used to mount the calibration piece during machining.

The dimensions of the disks and the sizes and configurations of the holes were essentially the same as those reported in the previous chapter on the theoretical stress analysis (see Figures 2 and 3).

Equipment

The following is a list of equipment and apparatus used in the experiment.

1. A stress freezing oven.

2. A 1000 watt chromalox heating element and a copper-constantan thermocouple.

3.   An automatic heating and cooling control unit designed and installed by Minneapolis-Honeywell, Inc. This unit is described in more detail later in this section.

4.   A 0° to 400°F mercury thermometer to make frequent checks of the oven temperature.

5.   A squirrel-cage induction motor of one quarter hp as a driving unit.

6.   A strobotac to determine the speed of rotation. It had a low range of 600 to 3700 rpm and a high range of 2400 to 14,500 rpm with separate adjustments for each range.

7.   A photoelastic bench with all its testing units, namely, po-larizer, analyzer, quarter-wave plates, separate monochromatic and white light sources, screen and camera.

The stress freezing oven was designed and fabricated. It was es-sentially a wooden box approximately 18 inches long, 15 inches deep, and 15 inches wide. It was lined with aluminum sheet 0.040 inch thick. Inside this aluminum sheet was a five-eighths inch layer of asbestos compound, and inside this a layer of aluminum foil. The purpose of this arrangement was principally to help minimize temperature differentials in the box as well as to provide insulation against heat loss and to protect the wood from any hot spot which might develop under some conditions.

The top of the oven, which was removable, had four holes to provide insertion of the thermocouple, the heating element, the thermometer, and the loading cable of the calibration piece. It also had two small grooved pulleys over which the light weight flexible metal loading cable from the calibration piece was led. Two opposite walls of the box were drilled at

seven and one-half inches from the top and seven and one-half inches from one end to receive ball bearings. A steel shaft, specially designed for the purpose, was inserted horizontally into the box and mounted in the bearings. The shaft had a stepped grooved pulley on one end, and the other end was threaded to receive a lock nut. It was designed to provide enough space to receive up to three disks, two small fan blades, a light compression spring, and suitable spacers (see Figures 4 and 5).

A 1000 watt chromalox heating element extending downward into the oven was used. A separate electric cable led from the head of this element to the control unit through a switch by means of which the heating power could be reduced to 500 watts. This feature was especially useful during the cooling process.

In order to record and control the temperature in the oven, a copper-constantan thermocouple was used. From time to time the thermocouple reading was checked against a mercury thermometer inserted in the oven. The agreement of the two readings was always within one degree Fahrenheit.

The heating and cooling of the oven was controlled by a unit designed by Minneapolis-Honeywell, Inc. The principal features of this unit consisted of

1. a Brown Electronic recording potentiometer with a range of 50°F to 350°F;

2. the control center containing the power switch to the heater itself, a reset rate control to determine the frequency of heating pulses, a proportional band control to determine the ratio of the length of the heating pulse to the total reset time, and an overriding manual heat con-
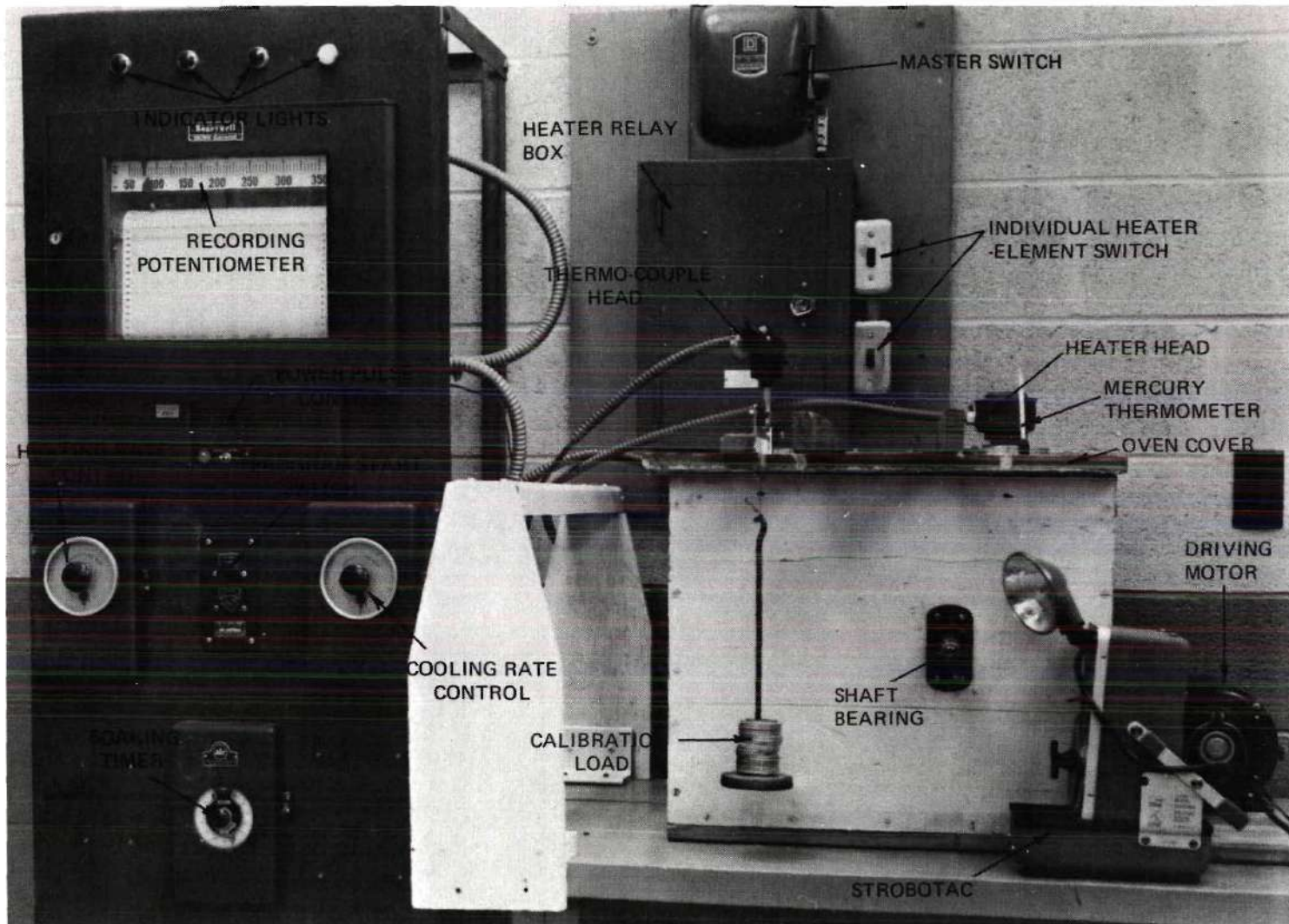
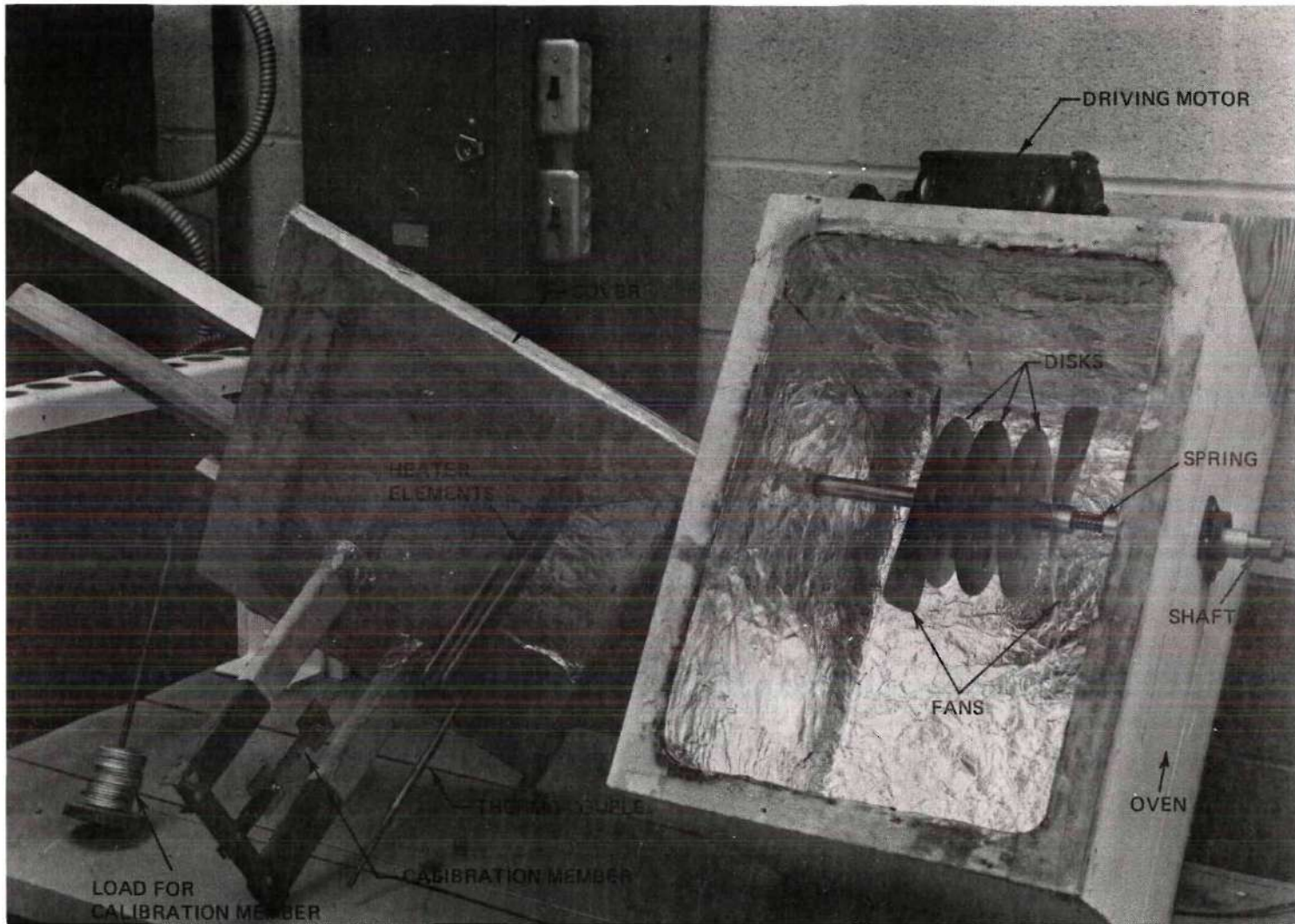Figure 4. Photograph of Stress Freezing Equipment

Figure 5. Details of Stress Freezing Oven and Cover

trol switch;

3. a program start switch;

4. heating and cooling rate controls with a temperature rate range
of from 0°F to 5°F per hour. When necessary, these controls were over-
ridden manually by moving the upper indicator on the potentiometer to the
desired temperature; and

5. a soaking timer relay which could be set for any period up to
480 minutes by turning the control knob on the timer.

Stress Freezing

The disk models were secured near the middle of the shaft by means
of spring loaded collars. On each side of the set of disks a small fan
blade was mounted to insure adequate circulation of air within the oven
and maintain uniform temperature throughout. The calibration member was
mounted in its loading rig which was a frame attached to the inside of the
top cover of the oven. The calibration member was loaded in direct ten-
sion. The shaft carrying the disks was driven by means of a light weight
V-belt from the motor.

The control unit was set to provide the following heating cycle.

1. Heating to 275°F in about 30 minutes, manually controlled.

2. Soaking at this temperature for 120 minutes.

3. Cooling to room temperature, 5°F per hour. The soaking and
cooling portions of the cycle were automatically controlled.

The three disks were run at 1680 rpm. After the runs were completed,
it was noted that the disk with the three-fourths inch noncentral holes
not only had a very poor fringe pattern, but it had been made from a bad
casting. Another disk with the same geometry was then used. Since the

fringe orders were rather low in all three specimens, the additional disk was run at 2670 rpm.

At the end of each run, when the temperature in the oven reached room temperature, the motor was stopped, and the disks and the calibration member were removed from the oven.

The disks and the calibration members were then given a light coat of rose oil, and the fringe pattern of each was photographed using monochromatic (green, 5461 Å) light in the polariscope (see Figures 6, 7, 8, and 9).

Stress Analysis from Photoelastic Data

The stresses in each disk tangent to the boundary of a noncentral hole in that disk were determined experimentally as follows.

From the calibration member, which was loaded in direct tension, the material fringe value was determined by the equation (Ref. 11, p. 161)

$$f = \frac{P}{2tn} \tag{67}$$

where

P is the applied load

t is the width of the member at the shank

n is the fringe order in the shank of the member as determined by
   the Tardy Compensation method (Ref. 14, p. 863).

For this member
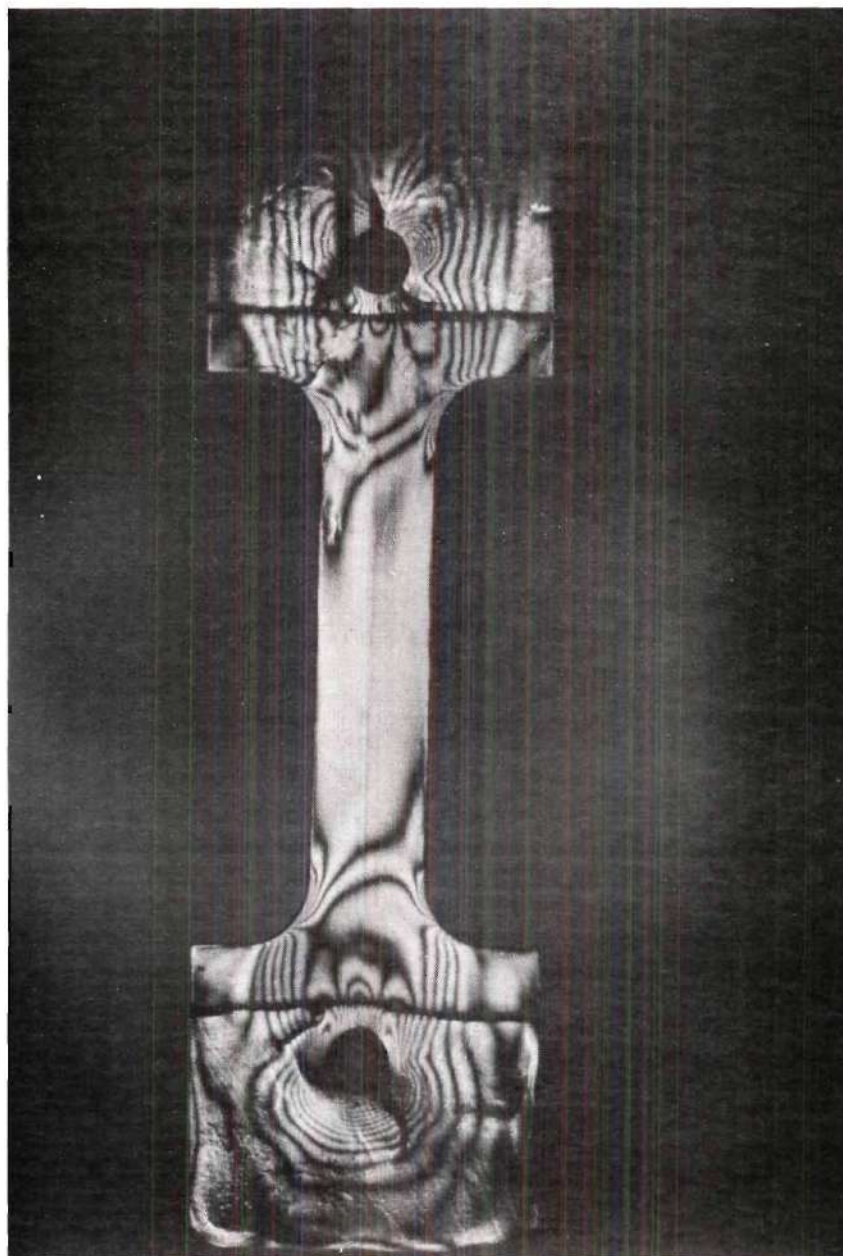
P = 4.00 lbs

t = 0.500 inch

n = 7.20

Figure 6. Frozen Stress Pattern in the Calibration Member

Figure 7.   Frozen Stress Pattern for Disk with 9/16 Inch Eccentric
Holes (rpm 1680)

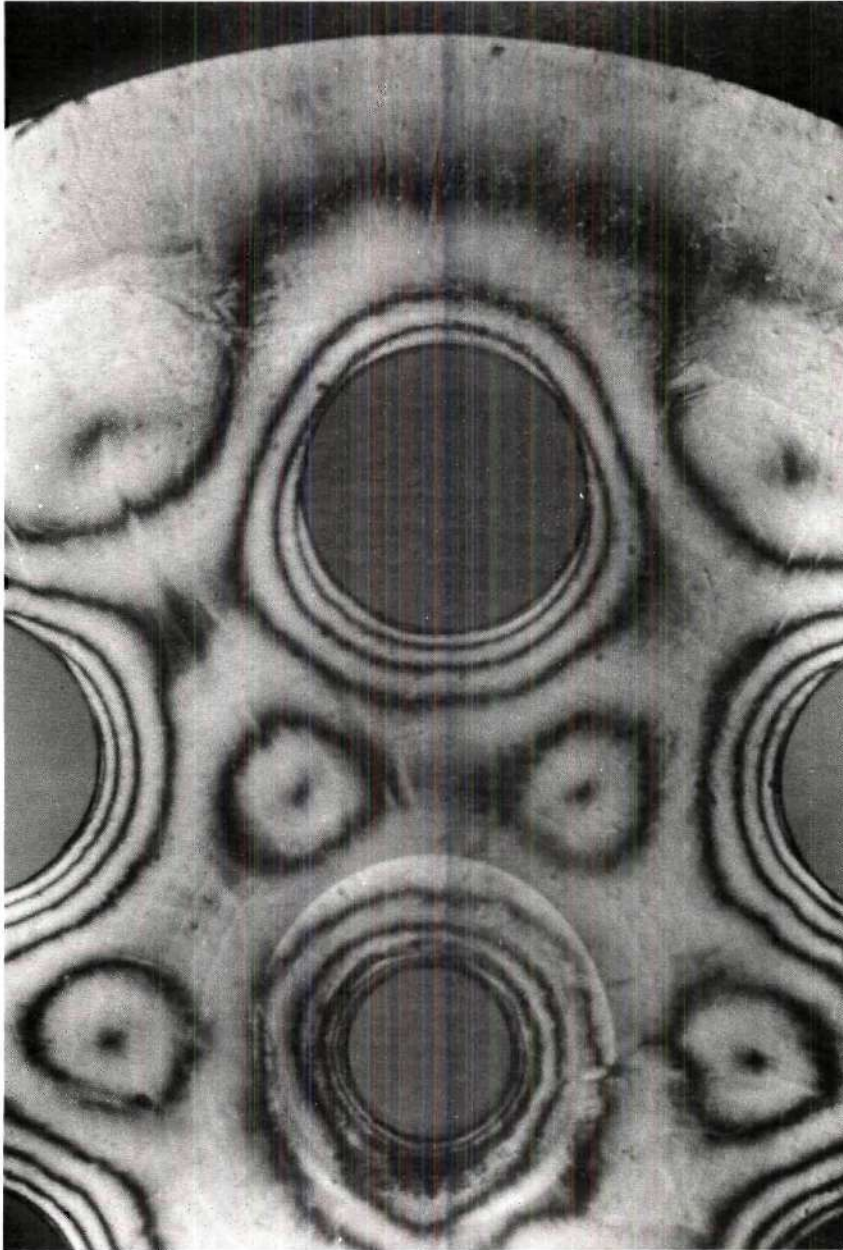Figure 8. Frozen Stress Pattern for Disk with 3/4 Inch Eccentric
Holes (rpm 2670)

Figure 9. Frozen Stress Pattern for Disk with 7/8 Inch Eccentric Holes (rpm 1680)

Therefore

$$f = \frac{4.00}{2(0.500)(7.20)}$$

$$= 0.555 \quad \text{lb per fringe inch}$$

At various stations in the disk around a noncentral hole, the values of $\sigma_\varphi - \sigma_\rho$ were determined by the familiar stress optic law (Ref. 11, p. 156)

$$\sigma_\varphi - \sigma_\rho = \frac{2nf}{h} \tag{68}$$

Since the noncentral holes are free from traction

$$\sigma_\rho = 0$$

and equation (68) gives

$$\sigma_\varphi = \frac{2nf}{h} \tag{69}$$

At a point on the hole boundary nearest the outside of the disk (i.e. at $= 0°$) for nine-sixteenth inch diameter holes,

$$n = 4.20$$

$$h = 0.320 \text{ inch}$$

$$\sigma_\varphi = \frac{2(4.20)(0.555)}{0.320}$$

$$= 14.58 \text{ psi}$$

In this way, the values of σ_φ around one half of the circumference of the noncentral holes (because the other half is symmetrical) in each disk were calculated and the results given in Tables 6, 7, and 8. In these tables, the values of σ_φ were rounded off to three significant figures.

Table 6. Photoelastic Stresses Around 9/16 Inch Diameter
Noncentral Holes, rpm 1680
(Other information as per Figures 2 and 7)

φ deg.	n	h inch	σ_φ psi
0	4.20	0.320	14.6
30	4.00	0.340	13.1
60	3.50	0.370	10.5
90	4.00	0.410	10.8
120	5.00	0.450	12.3
150	5.75	0.460	13.9
180	6.00	0.470	14.2

Table 7. Photoelastic Stresses Around 3/4 Inch Diameter
Noncentral Holes, rpm 2670
(Other information as per Figures 3 and 8)

φ deg.	n	h inch	σ_φ psi
0	8.75	0.268	36.2
30	8.00	0.270	32.9
60	7.00	0.300	26.0
90	8.00	0.330	27.0
120	10.00	0.355	31.2
150	12.00	0.385	34.6
180	12.50	0.395	35.2

Table 8. Photoelastic Stresses Around 7/8 Inch Diameter
          Noncentral Holes, rpm 1680
          (Other information as per Figures 3 and 9)

φ deg.	n	h inch	q_φ psi
0	3.5	0.240	16.2
30	3.25	0.250	14.4
60	3.00	0.300	11.1
90	4.00	0.370	12.0
120	5.50	0.394	15.5
135	5.75	0.398	16.0
150	5.50	0.400	15.3
180	5.25	0.415	14.1

The maximum stress at the edge of the central hole of the disk con-
taining nine-sixteenth inch diameter noncentral holes, from photoelastic
frange pattern is

$$\frac{2(7)(0.555)}{0.75} = 11.82 \text{ psi}$$

The corresponding stresses in the other disks are

$$\frac{2(17)(0.555)}{0.608} = 31.0 \text{ psi} \quad \text{(disk with 3/4 in. holes)}$$

and

$$\frac{2(7)(0.555)}{0.600} = 13.0 \text{ psi} \quad \text{(disk with 7/8 in. holes)}$$

These stresses are seen to be less than the maximum stresses at the edge
of a noncentral hole in the corresponding disks.

CHAPTER VI

DISCUSSION OF RESULTS

The mathematical analysis of the elastic stress problem pertaining
to a rotating tapered disk with noncentral holes is extremely difficult.
Even the analysis of the stress field in a uniform rotating disk with both
central hole and uniformly spaced noncentral holes is beset with algebraic
complication (Chapter VIII). In view of these, a recourse has been made
in utilizing the existing theoretical solutions of a tapered disk with a
central hole (Martin-Bisshopp) and a uniform disk with a symmetrical array
of noncentral holes (but no central hole)(Saito) and constructing therefrom
a solution that yields the stresses tangent to the boundaries around the
noncentral holes in a tapered disk of the type considered here. An accu-
rate analysis of this highly stressed zone is essential in order to design
the disk properly, and the method developed here appears to give extremely
good values. It should be pointed out that in the immediate region of a
hole the largest stresses occur at the hole boundary itself.

The results of the theoretical analysis presented in Chapter IV re-
veal a set of large stresses surrounding each eccentric hole in the tapered
disk. These stresses were subsequently confirmed experimentally by the
analysis of the corresponding photoelastic fringe patterns. Both the theo-
retical and photoelastic results are plotted in Figures 10, 11, and 12 for
comparison.

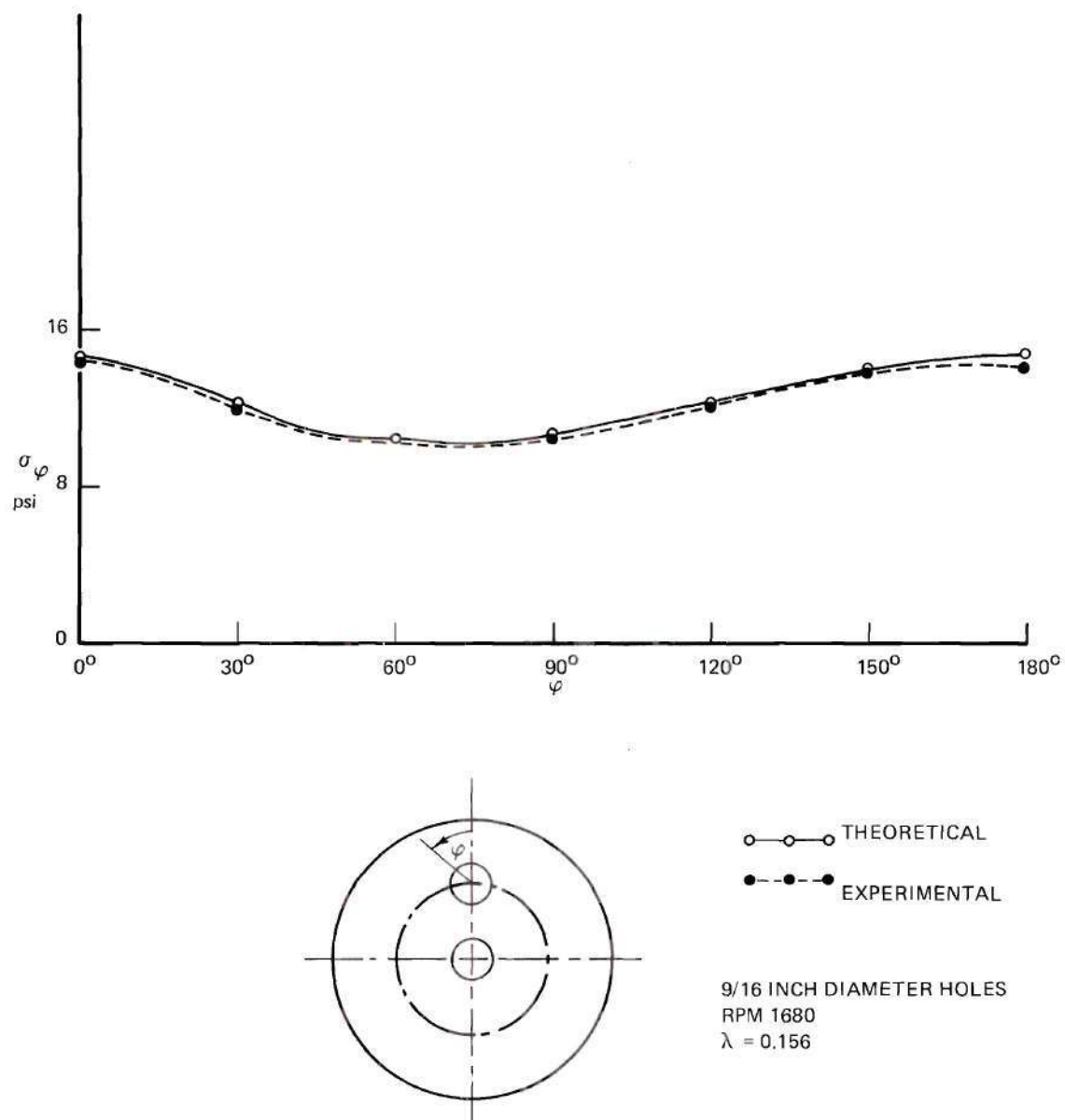From these graphs one can see that the theoretical stresses are

Figure 10.   Stresses Around 9/16 Inch Diameter Noncentral Holes
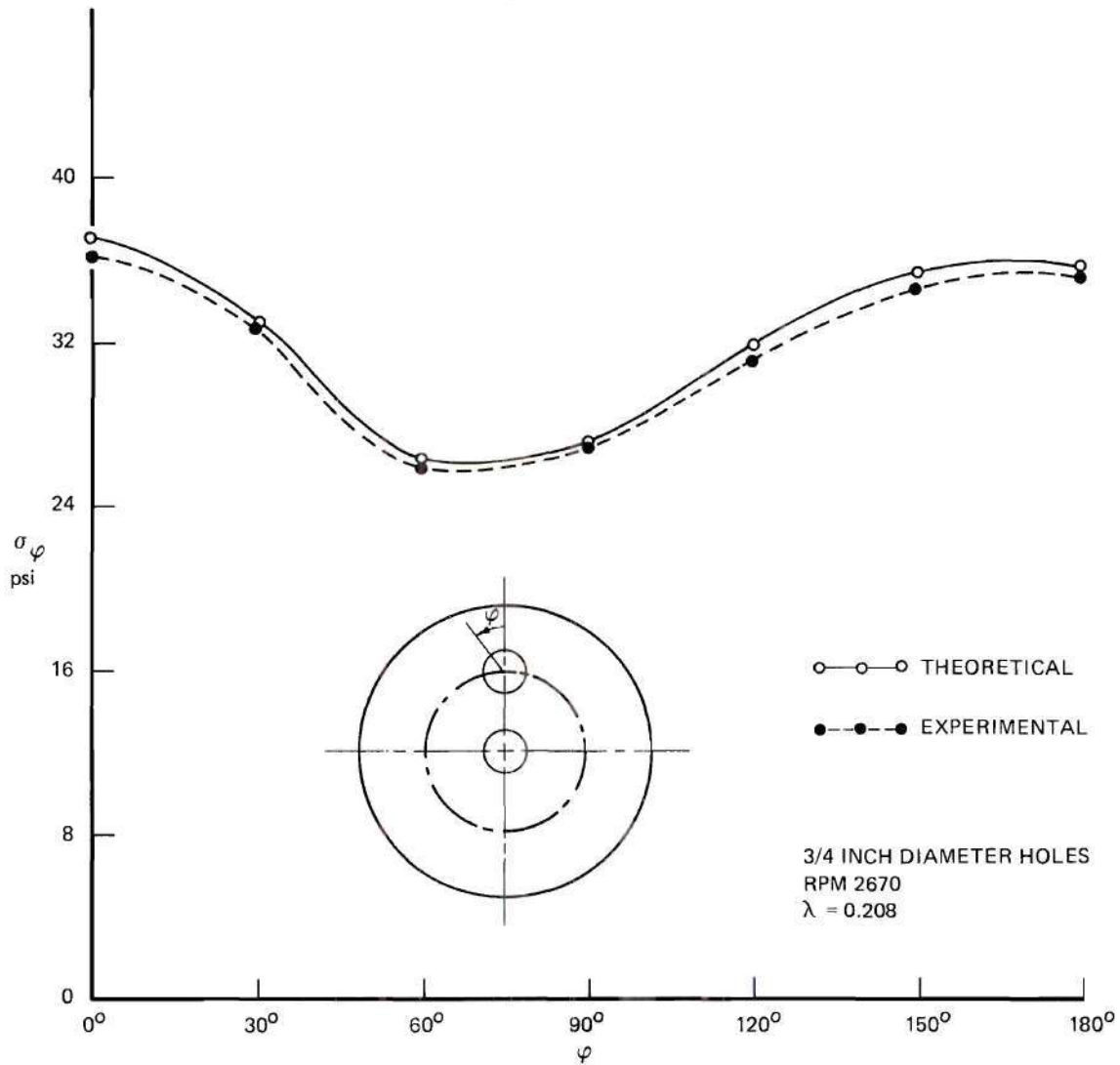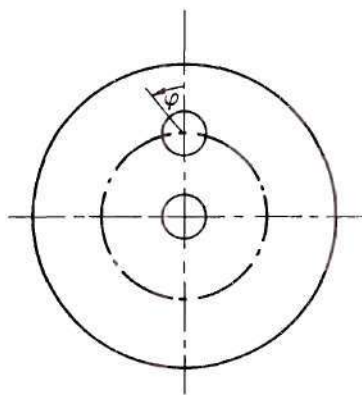in Rotating Tapered Disk

Figure 11.   Stresses Around 3/4 Inch Diameter Noncentral Holes
in Rotating Tapered Disk
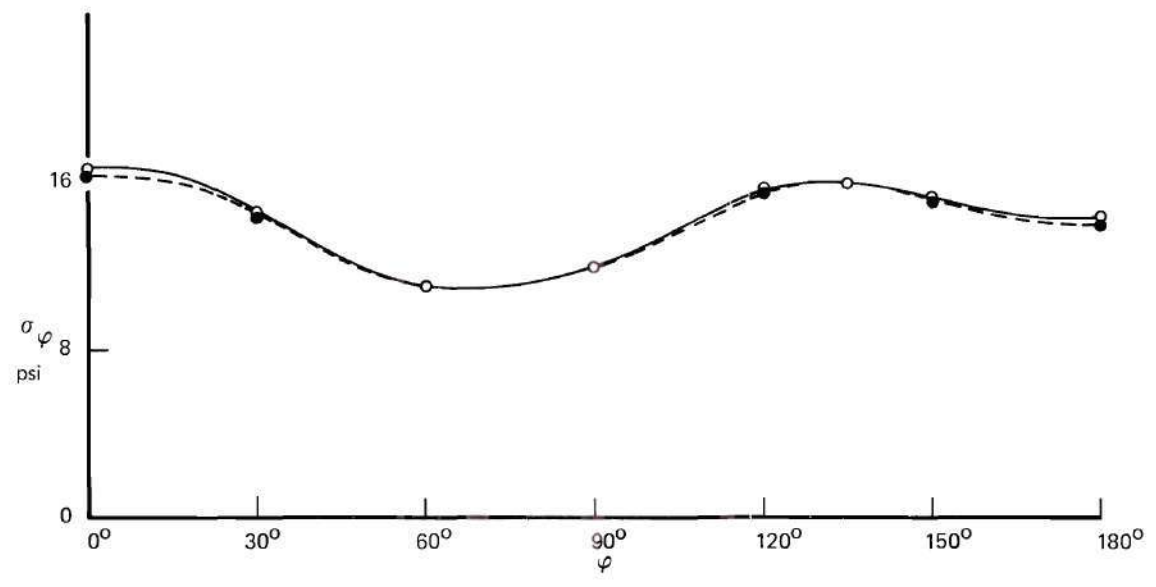
Figure 12.   Stresses Around 7/8 Inch Diameter Noncentral Holes
             in Rotating Tapered Disk

only slightly higher in magnitude than those determined experimentally and there is a remarkably close agreement between them throughout. For practical design of the disk based on strength, the stresses obtained from the theoretical analysis can be relied upon, as these appear to be conservative.

A comparison of the critical stresses at the edges of the central holes with those around a noncentral hole in the corresponding disk shows that the latter stresses are about 24 percent larger than those around the central hole. This suggests that the maximum stress occurring in the vicinity of the noncentral hole should be considered as a governing factor in the design. However, no such conclusion should be made in any case where the central hole has a keyway or a set of splines, or in cases where the total taper is considerably different from the approximately 12 degrees used here.

Due to machining difficulties, the taper in all the disks could not be maintained precisely the same, and there is a slight variation in their degrees of taper. Nevertheless, as the tapers used in all the disks are quite moderate, the following feature is remarkably common to all of them in spite of the variation in taper. The minimum stress is found to occur at values of φ between $60°$ and $75°$ and the stress level between $\varphi = 60°$ and $90°$ is about 33 percent less than the maximum stresses. The maximum stress points are mostly confined to the edges of the holes at $\varphi = 0°$ and $180°$, when the noncentral hole size is small, but, with the increase of diameter of the hole, the maximum stress position moves outward from $\varphi = 180°$ along the boundary to a point on the boundary near the minimum section between adjacent holes. When the diameter of the hole is

less than three-fourths inch (i.e. $\lambda < 0.2$), the stress peaks occur at $\varphi = 0°$ and at $180°$ as usual; but with increase of diameter, the stress at $\varphi = 180°$ decreases with a corresponding increase in stress at φ in between $120°$ to $180°$. The stress at $\varphi = 0°$ increases correspondingly. Notice that in case of seven-eighths inch diameter noncentral holes, the maximum stress position has shifted from $\varphi = 180°$ to $\varphi = 135°$. Even with three-fourths inch size holes, there is a marked tendency of a stress increase at φ in between $150°$ to $180°$. This is because, with the increase of the size of the holes, the material in the web region in between two neighboring holes as well as that between the outer edges of the disk and the hole is reduced with a corresponding increase of stress in these regions.

Before concluding this section, a word of caution is inserted here. The reader is advised against applying these results to disks with tapers appreciably beyond the tapers used in the present work without further investigation.

CHAPTER VII

CONCLUSIONS

The results of this investigation lead to the following conclusions.

1. Introduction of noncentral holes in rotating tapered disks creates local stresses which are, in general, larger than the stresses at the central hole.

2. For $\lambda < \frac{1}{4}$ (λ being the ratio of the noncentral hole size radius to its location radius) and for the values of taper used here (a total taper on the order of 12 degrees), the stress peaks in the disk occur at points on the noncentral hole boundary furthest from, and nearest to, the disk center; that is, at $\varphi = 0°$ and $\varphi = 180°$.

3. As λ increases beyond one fourth, the stress peak nearest the disk center, $\varphi = 180°$, shifts from that point toward the minimum section between noncentral holes, i.e. toward $\varphi = 120°$, with a corresponding decrease in the stress at $\varphi = 180°$.

4. The maximum stress around a noncentral hole in a tapered disk is a governing factor in the design of the disk and can be reliably and easily determined by means of the stress concentration factors developed in Chapter IV.

CHAPTER VIII

AN ANALYTICAL APPROACH TO THE CONSTRUCTION OF A STRESS

FUNCTION FOR A UNIFORM ROTATING DISK

WITH CENTRAL AND NONCENTRAL HOLES

In the following pages an analysis is given for the construction
of a stress function for a uniform rotating disk with a central hole and
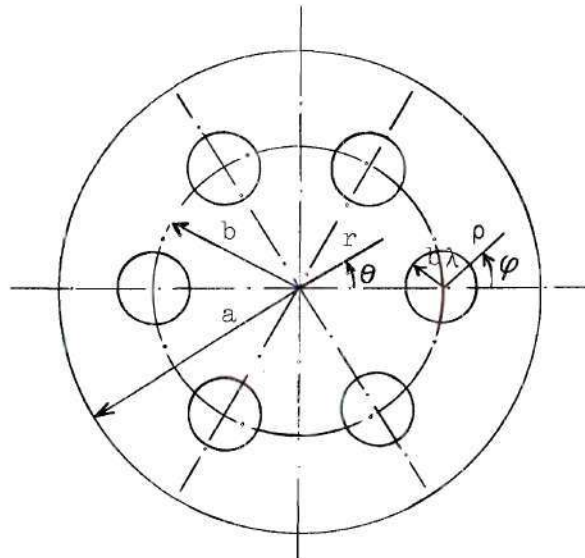a ring of equally spaced noncentral holes.

Figure 13.   Geometry of Rotating Uniform Disk
with Central and Noncentral Holes

A rotating disk with only a single hole at its center is a problem
in which both stresses and displacements are functions of r only. Intro-

duction of noncentral holes destroys the symmetry of the stress and strain fields and as a result stresses and strains become functions of both r and θ.

In the following analysis all of the usual assumptions regarding isotropy and homogeneity of the material and linearity of the stress and strain fields are made. The disk is assumed to be perfectly balanced and under the action of centrifugal force only. In addition, a condition of generalized plane stress is assumed to exist.

The quasi-static equations of equilibrium of the disk are obtained by considering a small element cut from the disk and balancing the forces acting on it in r and θ directions separately. These are

$$\frac{\partial}{\partial r}\left(r\,\sigma_r\right) + \frac{\partial\,\tau_{r\theta}}{\partial\theta} - \sigma_\theta = -\frac{\gamma}{g}\,\omega^2 r^2 \tag{70}$$

$$\frac{\partial}{\partial r}\left(r^2\,\tau_{r\theta}\right) + r\,\frac{\partial\sigma_\theta}{\partial\theta} = 0 \tag{71}$$

The equation of compatibility in this case is

$$\frac{\partial\gamma_{r\theta}}{\partial\theta} + r\,\frac{\partial^2\gamma_{r\theta}}{\partial r\,\partial\theta} - 2r\,\frac{\partial\epsilon_\theta}{\partial r} - r^2\,\frac{\partial^2\epsilon_\theta}{\partial r^2} + r\,\frac{\partial\epsilon_r}{\partial r} - \frac{\partial^2\epsilon_r}{\partial\theta^2} = 0 \tag{72}$$

The kinetmatic relationships are

$$\left.\begin{aligned}
\epsilon_r &= \frac{\partial u}{\partial r} \\[2mm]
\epsilon_\theta &= \frac{u}{r} + \frac{1}{r}\frac{\partial v}{\partial\theta} \\[2mm]
\gamma_{r\theta} &= \frac{1}{r}\frac{\partial u}{\partial\theta} + \frac{\partial v}{\partial r} - \frac{v}{r}
\end{aligned}\right\} \tag{73}$$

and the stress-strain relationships are

$$
\left.
\begin{aligned}
\epsilon_r &= \frac{1}{E} \left(\sigma_r - \nu\sigma_\theta \right) \\[2ex]
\epsilon_\theta &= \frac{1}{E} \left(\sigma_\theta - \nu\sigma_r \right) \\[2ex]
\gamma_{r\theta} &= \frac{2(1+\nu)}{E} \, \tau_{r\theta}
\end{aligned}
\right\}
\tag{74}
$$

The solution of equations (70) and (71) satisfying the compatibility and
the physical requirements of the problem can be conveniently achieved by
means of a stress function $\Phi(r,\theta)$. Before such a function is defined, let
the equilibrium equations be examined. Equation (70) has a body force
term on its right hand side. This force is a function of r only. The
occurrence of the radially varying body force in the equation of equili-
brium motivates one to start with a symmetrical problem: a problem per-
taining to the rotating uniform disk having the same dimensions and ge-
ometry as that of the original one, except the presence of the periodic
noncentral holes. The solution of this symmetrical problem, which is
easily obtained, is then modified to account for the noncentral holes of
the original disk in such a way that the proper boundary conditions are
established at the edges of the holes and at the inner and outer boundaries
of the disk.

With this idea in mind, the first step in the analysis is to imagine
the original disk not having the noncentral holes and to obtain a corres-
ponding solution for this. Since the stress distribution in case of the
disk without the noncentral holes is symmetrical with respect to the axis

of rotation of the disk, the stresses and displacements are functions of radius, r, only. The equations of equilibrium and compatibility associated with this case are

$$
\left.
\begin{aligned}
\frac{d}{dr}\left(r\sigma_{r_0}\right) - \sigma_{\theta_0} &= -\frac{\gamma}{g}\,\omega^2 r^2 \qquad \text{equilibrium} \\[2ex]
\epsilon_{\theta_0} - \epsilon_{r_0} + r\,\frac{d\epsilon_{\theta_0}}{dr} &= 0 \qquad \text{compatibility}
\end{aligned}
\right\} \tag{75}
$$

The subscript, o, is used to indicate the radial distribution of stresses and strains.

If a stress function $\Phi_0(r)$ is defined as follows

$$
\left.
\begin{aligned}
\sigma_{r_0} &= \frac{1}{r}\,\frac{d\Phi_0}{dr} \\[2ex]
\sigma_{\theta_0} &= \frac{d^2\Phi_0}{dr^2} + \frac{\gamma}{g}\,\omega^2 r^2
\end{aligned}
\right\} \tag{76}
$$

and equations (76) are introduced into equations (75), the first equation of (75) is found to be identically satisfied and the second one yields

$$
r^2\,\frac{d^3\Phi_0}{dr^3} + r\,\frac{d^2 r_0}{dr^2} - \frac{d\Phi_0}{dr} + (3+\nu)\,\frac{\gamma}{g}\,\omega^2 r^3 = 0 \tag{77}
$$

the general solution of which is

$$
\Phi_0(r) = C_1 + C_2\,\log r + C_3 r^2 - \frac{3+\nu}{32}\,\frac{\gamma}{g}\,\omega^2 r^4 \tag{78}
$$

where C_1, C_2, and C_3 are arbitrary constants. Since C_1 does not affect the stress system, equations (76), it may be dropped from equation (78). Thus

$$\Phi_0(r) = C_2 \log r + C_3 r^2 - \frac{3+\nu}{32} \frac{\gamma}{g} \omega^2 r^4 \tag{79}$$

In view of equation (77), the stresses are given by the following expressions.

$$\left.\begin{aligned} \sigma_{r_0} &= \frac{C_2}{r^2} + 2C_3 - \frac{3+\nu}{8} \frac{\gamma}{g} \omega^2 r^2 \\[2mm] \sigma_{\theta_0} &= -\frac{C_2}{r^2} + 2C_3 - \frac{1+3\nu}{8} \frac{\gamma}{g} \omega^2 r^2 \end{aligned}\right\} \tag{80}$$

Using the boundary conditions

$$\sigma_{r_0} = 0 \quad \text{at} \quad r = d \quad \text{and} \quad r = a$$

one obtains

$$\left.\begin{aligned} C_2 &= -\frac{3+\nu}{8} \frac{\gamma}{g} \omega^2 a^2 d^2 \\[2mm] C_3 &= \frac{3+\nu}{16} \frac{\gamma}{g} \omega^2 (a^2+d^2) \end{aligned}\right\} \tag{81}$$

In view of these values, equations (80) yield

$$\left.\begin{aligned} \sigma_{r_0} &= \frac{3+\nu}{8} \frac{\gamma}{g} \omega^2 \left(a^2+d^2 - \frac{a^2 d^2}{r^2} - r^2\right) \\[2mm] \sigma_{\theta_0} &= \frac{3+\nu}{8} \frac{\gamma}{g} \omega^2 \left(a^2+d^2 + \frac{a^2 d^2}{r^2} - \frac{1+3\nu}{3+\nu} r^2\right) \end{aligned}\right\} \tag{82}$$

which are recognized to be the stresses in a rotating uniform disk with a

central hole.

When the disk is perforated by the noncentral holes, the stress function $\Phi_0(r)$ leaves boundary tractions on the edges of the holes, thus not giving the true solution.

Therefore the main concern, hereafter, will be to construct two correcting stress functions with the help of the equations (70) (without body force term[*]), (71), and (72), which will eliminate the boundary tractions produced on the holes by $\Phi_0(r)$ and which at the same time will not violate the traction free situations on the inner and outer edges of the disk.

Let Φ_c be some correcting stress function, which is defined as follows.

$$\left.\begin{array}{l} \sigma_r = \dfrac{1}{r}\dfrac{\partial \Phi_c}{\partial r} + \dfrac{1}{r^2}\dfrac{\partial^2 \Phi_c}{\partial \theta^2} \\[2mm] \sigma_\theta = \dfrac{\partial^2 \Phi_c}{\partial r^2} \\[2mm] \tau_{r\theta} = \dfrac{1}{r^2}\dfrac{\partial \Phi_c}{\partial \theta} - \dfrac{1}{r}\dfrac{\partial^2 \Phi_c}{\partial r\,\partial \theta} \end{array}\right\} \quad (83)$$

Φ_c defined as such, then, satisfies the equations of equilibrium (70,71) (without body force term) identically and reduces the compatibility equation (72) to

$$\left(\dfrac{\partial^2}{\partial r^2} + \dfrac{1}{r}\dfrac{\partial}{\partial r} + \dfrac{1}{r^2}\dfrac{\partial^2}{\partial \theta^2}\right)\left(\dfrac{\partial^2 \Phi_c}{\partial r^2} + \dfrac{1}{r}\dfrac{\partial \Phi_c}{\partial r} + \dfrac{1}{r^2}\dfrac{\partial^2 \Phi_c}{\partial \theta^2}\right) = 0 \quad (84)$$

---

[*]The body force term is already taken care of by Φ_0.

In view of the physical nature of the problem, the first correcting stress function, $\Phi_{c_1}(r,\theta)$, should be such that it will relate to the disk with a central hole and have a period $\frac{2\pi m}{k}$ (m=0,1,2, . . .,k-1), that is, its values will recur when rotated about the center of the disk through angles $\frac{2\pi m}{k}$, k being the number of noncentral holes. This is necessary, because the periodic distribution of the noncentral holes imparts periodicity to the stress and displacement fields in the disk. Further $\Phi_{c_1}(r,\theta)$ has to be chosen with the added restrictions that it must be an even function of θ and be such that it would lead to a single valued displacement field in the complete disk. Finally, it is desired that $\Phi_{c_1}(r,\theta)$ should be biharmonic as it has to satisfy the equation (84). All these conditions are identically fulfilled when $\Phi_{c_1}(r,\theta)$ has the following form (Ref. 37, p. 116):

$$\Phi_{c_1}(r,\theta) = \sum_{n=1}^{\infty} (A_n\, r^{2-nr} + B_n\, r^{-nk} + A_n'\, r^{2+nk} + B_n'\, r^{nk}) \cos nk\theta \quad (85)$$

The second correcting stress function $\Phi_{c_2}(r,\theta)$ is associated with a ring of k equally spaced noncentral holes arranged around the center of the disk. It should be of such a form that it would provide appropriate singularity at the center of each noncentral hole. Like the first correcting stress function, $\Phi_{c_2}(r,\theta)$ is required to be an even biharmonic function (as equation (84) has to be satisfied) leading to a single valued displacement field. It should also have enough arbitrariness such that in combination with $\Phi_{c_1}(r,\theta)$ it will be able to equilibrate the stress state left over by $\Phi_0(r)$ along the hole boundaries, without violating the traction free situations on the inner and outer boundaries of the disk.

The stress function $\Phi_{c_2}(r,\theta)$ satisfying all these imposed restrictions can be written down in its best possible form with the help of complex variables. Define the plane of the disk by the complex variable

$$z = r\, e^{i\theta} \tag{86}$$

where the central hole is located at $r = 0$

and the ring of k circular holes of equal radii, $b\lambda$, whose centers are located at the points given by

$$z = b\, e^{2im\pi/k}, \quad \text{where} \quad m=0,1,2,\ldots,k-1 \tag{87}$$

b is the location radius and λ is a nondimensional parameter (see Figure 13).

Now the structure of $\Phi_{c_2}(r,\theta)$ is established by considering a class of harmonic functions with logarithmic singularity at each center as derived by Howland (18).

Howland defined

$$W_0 = U_0 - i\, V_0$$

$$= - \log \prod_{m=0}^{k-1} (z - b\, e^{2im\pi/k})$$

$$= - \log (z^k - b^k) \tag{88}$$

the real part of which is periodic.

Its derivatives, which will be represented by

$$W_s = U_s - i\, V_s$$

$$= \frac{b^s}{(s-1)!} \frac{d^s W_0}{db^s} \tag{89}$$

represent a general set of harmonic functions U_s and V_s, for all positive integral values of s, each W_s having a pole of order s at the centers of the noncentral holes defined by equation (87) and analytic elsewhere. The need for an even biharmonic function is achieved by taking the terms U_s and $r^2 U_s$ into account. Thus

$$\Phi_{C_2}(z) = C_{30} U_0 + \sum_{s=1}^{\infty} [C_{1s} r^2 U_s + C_{3s} U_s] \tag{90}$$

The constant C_{10} is taken equal to zero as $r^2 U_0$ involves $r^2 \log r$ which leads to a multivalued displacement field.

It is necessary to express Φ_{C_2} in terms of the coordinates (r,θ). Due to singularities on the circle $|z| = b$, the expansion of W_0 and W_s into power series is different depending on whether $|z| > b$ or $|z| < b$.

For $|z| > b$

$$W_0 = -k \log z + \sum_{n=1}^{\infty} \frac{1}{n} \left(\frac{b}{z}\right)^{nk} \tag{91}$$

and for $|z| < b$

$$W_0 = \pi i - k \log b + \sum_{n=1}^{\infty} \frac{1}{n} \left(\frac{z}{b}\right)^{nk} \tag{92}$$

Also, for $|z| > b$

$$W_s = k \sum_{n=1}^{\infty} \binom{nk-1}{s-1}\left(\frac{b}{z}\right)^{nk} \tag{93}$$

and for $|z| < b$

$$W_S = (-1)^S \, k \sum_{n=0}^{\infty} \binom{nk+s-1}{s-1}\left(\frac{z}{b}\right)^{nk} \tag{94}$$

where $\binom{s}{n} = \dfrac{s!}{n!(s-n)!}$, the binomial coefficient which is zero for $n > s$.

The real parts of W_O and W_S are then

$$\left.\begin{aligned} U_O &= -k \log r + \sum_{n=1}^{\infty} \frac{1}{n}\left(\frac{b}{r}\right)^{nk} \cos nk\theta \\[2em] U_S &= k \sum_{n=1}^{\infty} \binom{nk-1}{s-1}\left(\frac{b}{r}\right)^{nk} \cos nk\theta \end{aligned}\right\} \quad \text{for } r > b \tag{95}$$

and

$$\left.\begin{aligned} U_O &= -k \log b + \sum_{n=1}^{\infty} \frac{1}{n}\left(\frac{r}{b}\right)^{nk} \cos nk\theta \\[2em] U_S &= (-1)^S \, k \sum_{n=0}^{\infty} \binom{nk+s-1}{s-1}\left(\frac{r}{b}\right)^{nk} \cos nk\theta \end{aligned}\right\} \quad \text{for } r < b \tag{96}$$

When the expansions (95) and (96) are introduced into equation (90), one obtains

$$\Phi_{C_2}(r,\theta) = -C_{30} \, k \log r + \sum_{n=1}^{\infty} (M_{1n} r^2 + M_{3n}) \, r^{-nk} \cos nk\theta \tag{97}$$

$$\text{for } r > b$$

and

$$\Phi_{C_2}(r,\theta) = -C_{30} \, k \log b + kr^2 \sum_{n=1}^{\infty} (-1)^n C_{1n} \tag{98}$$

$$+ \sum_{n=1}^{\infty} (M_{2n} r^2 + M_{4n}) \, r^{nk} \cos nk\theta$$

$$\text{for } r < b$$

where

$$M_{1n} = k\, b^{nk} \sum_{s=1}^{nk} \binom{nk-1}{s-1}\, C_{1s} \tag{99}$$

$$M_{2n} = k\, b^{-nk} \sum_{s=1}^{\infty} (-1)^s \binom{nk+s-1}{s-1}\, C_{1s} \tag{100}$$

$$M_{3n} = \frac{b^{nk}}{n}\, C_{30} + k\, b^{nk} \sum_{s=1}^{nk} \binom{nk-1}{s-1}\, C_{3s} \tag{101}$$

$$M_{4n} = \frac{b^{-nk}}{n}\, C_{30} + k\, b^{-nk} \sum_{s=1}^{\infty} (-1)^s \binom{nk+s-1}{s-1}\, C_{3s} \tag{102}$$

Now, when equations (97) and (98) are combined separately with the sum of equations (85) and (79), and equation (81) is recalled, the complete stress function, $\Phi = \Phi_0(r) + \Phi_{c_1}(r,\theta) + \Phi_{c_2}(r,\theta)$ is obtained. Thus

$$\Phi(r,\theta) = -\frac{3+\nu}{32}\frac{\gamma}{g}\,\omega^2 \{4a^2 d^2 \log r - 2(a^2+d^2)\,r^2 + r^4\} \tag{103}$$

$$- C_{30}\, k \log r + \sum_{n=1}^{\infty} (A_n r^2 + B_n + M_{1n} r^2 + M_{3n})\, r^{-nk} \cos nk\theta$$

$$+ \sum_{n=1}^{\infty} (A_n' r^2 + B_n')\, r^{nk} \cos nk\theta, \quad \text{for } r > b$$

and

$$\Phi(r,\theta) = -\frac{3+\nu}{32}\frac{\gamma}{g}\,\omega^2 \{4a^2 d^2 \log r - 2(a^2+d^2)\,r^2 + r^4\} \tag{104}$$

$$- C_{30}\, k \log b + k r^2 \sum_{n=1}^{\infty} (-1)^n C_{1n} + \sum_{n=1}^{\infty} (A_n r^2 + B_n)$$

$$\times\, r^{-nk} \cos nk\theta + \sum_{n=1}^{\infty} (A_n' r^2 + B_n' + M_{2n} r^2 + M_{4n})\, r^{nk} \cos nk\theta$$

$$\text{for } r < b$$

The associated radial and shear stresses are

$$\sigma_r = \frac{1}{r} \frac{\partial \Phi}{\partial r} + \frac{1}{r^2} \frac{\partial^2 \Phi}{\partial \theta^2} \tag{105}$$

$$= \frac{3+\nu}{8} \frac{\gamma}{g} \omega^2 \left(a^2+d^2 - \frac{a^2 d^2}{r^2} - r^2\right)$$

$$- C_{30} k \frac{1}{r^2} + \sum_{n=1}^{\infty} \left[(2-nk-n^2k^2)(A_n+M_{1n}) - \frac{1}{r^2}(nk+n^2k^2)(B_n+M_{3n}) \right]$$

$$\times r^{-nk} \cos nk\theta + \sum_{n=1}^{\infty} \left[(2+nk-n^2k^2) A_n' + \frac{1}{r^2}(nk-n^2k^2) B_n' \right]$$

$$\times r^{nk} \cos nk\theta \ , \quad \text{for} \quad r > b$$

$$\tau_{r\theta} = \frac{1}{r^2} \frac{\partial \Phi}{\partial \theta} - \frac{1}{r} \frac{\partial^2 \Phi}{\partial r \, \partial \theta} \tag{106}$$

$$= \sum_{n=1}^{\infty} \left[(nk-n^2k^2)(A_n+M_{1n}) - (nk+n^2k^2) \frac{1}{r^2}(B_n+M_{3n}) \right] r^{-nk} \sin nk\theta$$

$$+ \sum_{n=1}^{\infty} \left[(nk+n^2k^2) A_n' + (n^2k^2-nk) \frac{1}{r^2} B_n' \right] r^{nk} \sin nk\theta$$

$$\text{for} \quad r > b$$

and

$$\sigma_r = \frac{3+\nu}{8} \frac{\gamma}{g} \omega^2 \left(a^2+d^2 - \frac{a^2 d^2}{r^2} - r^2\right) \tag{107}$$

$$+ 2k \sum_{n=1}^{\infty} (-1)^n C_{1n} + \sum_{n=1}^{\infty} \left[(2-nk-n^2k^2) A_n - \frac{1}{r^2}(nk+n^2k^2) B_n \right]$$

$$\times r^{-nk} \cos nk\theta + \sum_{n=1}^{\infty} \left[(2+nk-n^2k^2)(A_n'+M_{2n}) + \frac{1}{r^2}(nk-n^2k^2) \right.$$

$$\times \left. (B_n'+M_{4n}) \right] r^{nk} \cos nk\theta, \quad \text{for} \quad r < b$$

$$\tau_{r\theta} = \sum_{n=1}^{\infty} \left[(nk - n^2 k^2) A_n - (nk + n^2 k^2) \frac{1}{r^2} B_n \right] r^{-nk} \sin nk\theta \qquad (108)$$

$$+ \sum_{n=1}^{\infty} \left[(nk + n^2 k^2)(A_n' + M_{2n}) + (n^2 k^2 - nk) \frac{1}{r^2} (B_n' + M_{4n}) \right] r^{nk} \sin nk\theta$$

for $r < b$

It is required that the boundaries at $r=a$ and $r=d$ must have zero radial and shear stresses. As a result of this, the following equations are obtained.

$$C_{30} = 0 \qquad (109)$$

$$\sum_{n=1}^{\infty} (-1)^n C_{1n} = 0 \qquad (110)$$

$$(2 - nk - n^2 k^2) a^{-2nk} A_n - (nk + n^2 k^2) a^{-2(1+nk)} B_n + (2 + nk - n^2 k^2) A_n'$$

$$+ (nk - n^2 k^2) a^{-2} B_n' = (n^2 k^2 + nk - 2) a^{-2nk} M_{1n} + (n^2 k^2 + nk) \qquad (111)$$

$$\times \ a^{-2(1+nk)} M_{3n}$$

$$(nk - n^2 k^2) a^{-2nk} A_n - (nk + n^2 k^2) a^{-2(1+nk)} B_n + (nk + n^2 k^2) A_n'$$

$$+ (n^2 k^2 - nk) a^{-2} B_n' = (n^2 k^2 - nk) a^{-2nk} M_{1n} + (n^2 k^2 + nk) \qquad (112)$$

$$\times \ a^{-2(1+nk)} M_{3n}$$

$$(2-nk-n^2k^2) \; d^{-2nk} \; A_n \; - \; (nk+n^2k^2) \; d^{-2(1+nk)} \; B_n \; + \; (2+nk-n^2k^2) \; A_n'$$

$$+ \; (nk-n^2k^2) \; d^{-2} \; B_n' = (n^2k^2-nk-2) \; M_{2n} \; + \; (n^2k^2-nk) \; d^{-2} \; M_{4n} \qquad (113)$$

$$(nk-n^2k^2) \; d^{-2nk} \; A_n \; - \; (nk+n^2k^2) \; d^{-2(1+nk)} \; B_n \; + \; (nk+n^2k^2) \; A_n'$$

$$+ \; (n^2k^2-nk) \; d^{-2} \; B_n' = (-nk-n^2k^2) \; M_{2n} \; + \; (nk-n^2k^2) \; d^{-2} \; M_{4n} \qquad (114)$$

M_{1n}, M_{2n}, M_{3n}, and M_{4n} are related to C_{1s} and C_{3s} by equations (99), (100), (101), and (102). Hence, it is obvious from equations (111), (112), (113), and (114) that A_n, B_n, A_n', and B_n' are also related to C_{1s} and C_{3s}. The determination of C_{1s} and C_{3s} will determine the constants A_n, B_n, A_n', and B_n'; therefore, it is necessary to ascertain the constants C_{1s} and C_{3s} from the conditions placed on the stresses at the boundaries of the periodic holes.

In order to make it feasible, all the stress functions derived so far must be transformed in terms of the coordinates (ρ, φ), which are referred to the center of one of the noncentral holes (see Figure 13). In other words, it is necessary to have

$$\Phi(\rho,\varphi) = \Phi_0(\rho,\varphi) + \Phi_{c_1}(\rho,\varphi) + \Phi_{c_2}(\rho,\varphi) \qquad (115)$$

In this context, reference is again made to Howland (18) who has derived the harmonic functions U_s ($s=0,1,2,\ldots$) corresponding to the coordinates (ρ, φ) as follows.

Ir is seen (refer to equations (87) and (88)) that a function with logarithmic singularity at the points

$$z = b\ e^{2im\pi/k}\ ,\ m=0,1,2,\ \cdot\ \cdot\ \cdot,k-1$$

is

$$W_0 = -\log \prod_{m=0}^{k-1} (z - b\ e^{2im\pi/k})$$

$$= -\log (z^k - b^k)$$

Now writing

$$z-b = b\zeta = b\rho\ e^{i\varphi}\quad (\text{see Figure 13}) \tag{116}$$

one has, apart from a constant

$$W_0 = -\log \zeta - \sum_{n=1}^{k-1} \log (1+u_m\zeta) \tag{117}$$

where

$$\frac{1}{u_m} = 1 - e^{2im\pi/k} \tag{118}$$

and u_m is a root of

$$(u-1)^k - u^k = 0 \tag{119}$$

Expansion of the logarithmic terms gives

$$W_0 = -\log \zeta + \sum_{n=1}^{\infty} (-1)^n\ (^n\alpha_0)\ \zeta^n \tag{120}$$

where

$$^n\alpha_0 = \frac{1}{n} \sum_{m=1}^{k-1} u_m^n\ ,\quad \text{that is,}\ \frac{1}{n}\ \text{times the sum of the } n^{th}\ \text{power of the}$$

roots of equation (119). When this is rewritten as

$$n_{\alpha_0} = \frac{\chi_n}{n} \,, \quad \text{where} \quad \chi_n = \sum_{m=1}^{k-1} u_m^n \tag{121}$$

one finds from equation (118)

$$\chi_n = \frac{1}{2^n} \sum_{m=1}^{k-1} (i\ e^{-m\pi i/k}\ \operatorname{cosec} \tfrac{m\pi}{k})^n$$

$$= \frac{1}{2^{n-1}} \sum_{m=1}^{\frac{1}{2}(k-1)} \cos n\pi\, (\tfrac{1}{2} - \tfrac{m}{k})\ \operatorname{cosec}^n \tfrac{m\pi}{k} \,, \quad \text{for } k \text{ odd} \tag{122}$$

$$= \frac{1}{2^n} + \frac{1}{2^{n-1}} \sum_{m=1}^{\frac{1}{2}k-1} \cos n\pi\, (\tfrac{1}{2} - \tfrac{m}{k})\ \operatorname{cosec}^n \tfrac{m\pi}{k}, \quad \text{for } k \text{ even} \tag{123}$$

so that χ_n can be calculated for any given pair of values of k and n.

The functions derived from equation (88) by successive differentiation with respect to b must recur after rotations about the center of the disk through angles $\frac{2m\pi}{k}$. Writing equation (88) again in the form

$$W_0 = -\log (z-b) - \sum_{m=1}^{k-1} \log (z-b\ e^{2m\pi i/k}) \tag{124}$$

and defining

$$W_s = \frac{b^s}{(s-1)!} \frac{d^s W_0}{db^s}$$

one has, for $s \geqq 1$

$$W_s = \frac{1}{\zeta^s} + \sum_{m=1}^{k-1} \frac{(u_m-1)^s}{(1+u_m\zeta)^s} \tag{125}$$

(continued)

(equation (125) continued)

$$= \frac{1}{\zeta^s} + \sum_{m=1}^{k-1} (u_m-1)^s \sum_{p=0}^{\infty} (-1)^p \binom{p+s-1}{p} (u_m\zeta)^p$$

$$= \frac{1}{\zeta^s} + \sum_{p=0}^{\infty} (-1)^p \; {}^p\alpha_s \; \zeta^p$$

where

$${}^p\alpha_s = \sum_{m=1}^{k-1} (u_m-1)^s \binom{p+s-1}{p} u_m^p \tag{126}$$

$$= \binom{p+s-1}{p} \sum_{r=0}^{s} (-1)^r \binom{s}{r} \chi_{p+s-r}$$

$$= \binom{p+s-1}{p} \Delta^s \chi_p$$

in which $\Delta^s\chi_p$ is the sth finite difference of the series χ_p, χ_{p+1}, χ_{p+2}, ...

From equation (119) by binomial expansion

$$u^{p+mk} = \sum_{r=0}^{mk} (-1)^r \binom{mk}{r} u^{p+mk-r} \tag{127}$$

where m is a positive integer. Summing over the roots, one has

$$\chi_{n+mk} = \sum_{r=0}^{mk} (-1)^r \binom{mk}{r} \chi_{p+mk-r} \tag{128}$$

$$= \Delta^{mk} \chi_p$$

so that all the coefficients ${}^p\alpha_s$ can be found from the values of χ_p and its first $(k-1)^{th}$ difference.

When W_s is split into its real and imaginary parts and $\zeta = \rho \, e^{i\varphi}$ is introduced, it is found that the real parts yield

$$U_O = - \log \rho + \sum_{p=1}^{\infty} (-1)^p \, {}^p\alpha_0 \, \rho^p \cos p\varphi \tag{129}$$

$$U_s = \frac{\cos s\varphi}{\rho^s} + \sum_{p=0}^{\infty} (-1)^p \, {}^p\alpha_s \, \rho^p \cos p\varphi \tag{130}$$

With the help of relation (116), the following transformations are obtained

$$r^2 = z\bar{z} = b^2 \, (1+\rho \, e^{i\varphi})(1+\rho \, e^{-i\varphi})$$

$$r^2 = b^2 \, (1+\rho^2 + 2\rho \cos\varphi) \tag{131}$$

$$r^4 = b^4 \, [1+4\rho^2 + \rho^4 + 4\rho \, (1+\rho^2) \cos\varphi + 2\rho^2 \cos 2\varphi] \tag{132}$$

$$\log r = \text{Real} \, (\log z) \tag{133}$$

$$= \text{Real} \log b \, (1+\rho \, e^{i\varphi})$$

$$= \log b + \sum_{p=1}^{\infty} (-1)^{p+1} \frac{\rho^p}{p} \cos p\varphi$$

$$r^{nk} \cos nk\theta = \text{Real} \, (z^{nk}) \tag{134}$$

$$= b^{nk} \sum_{p=0}^{nk} \binom{nk}{p} \rho^p \cos p\varphi$$

$$r^{-nk} \cos nk\theta = \text{Real} \, (z^{-nk}) \tag{135}$$

$$= b^{-nk} \sum_{p=0}^{\infty} (-1)^p \binom{nk+p-1}{p} \rho^p \cos p\varphi$$

As C_{30} is zero, equation (109), one obtains from equation (90), in view of equation (130)

$$\Phi_{C_2}(\rho,\varphi) = \sum_{s=1}^{\infty} [C_{1s}b^2 (1+\rho^2 + 2\rho \cos\varphi) + C_{3s}][\rho^{-s} \cos s\varphi \qquad (136)$$

$$+ \sum_{p=0}^{\infty} (-1)^p {}^p\alpha_s \rho^p \cos p\varphi]$$

Also in view of the transformations (131), (134), and (135), the stress function defined by equation (85) is now rewritten in terms of (ρ,φ) coordinates as follows.

$$\Phi_{C_1}(\rho,\varphi) = \sum_{n=1}^{\infty} [\{A_n b^2 (1+\rho^2 + 2\rho \cos\varphi) + B_n\} b^{-nk} \qquad (137)$$

$$\times \sum_{p=0}^{\infty} (-1)^p \binom{nk+p-1}{p} \rho^p \cos p\varphi] + \sum_{n=1}^{\infty} [\{A_n' b^2$$

$$\times (1+\rho^2 + 2\rho \cos\varphi) + B_n'\} b^{nk} \sum_{p=0}^{nk} \binom{nk}{p} \rho^p \cos p\varphi]$$

Finally, with the help of the transformations (131), (132), and (133), and in view of equation (81), the stress function $\Phi_0(r)$, equation (79), is transformed into (ρ,φ) coordinates as follows.

$$\Phi_0(\rho,\varphi) = - \frac{3+\nu}{32} \frac{\gamma}{g} \omega^2 [4a^2d^2 \{ \log b + \sum_{p=1}^{\infty} (-1)^{p+1} \frac{\rho^p}{p} \cos p\varphi\} \qquad (138)$$

$$- 2(a^2+d^2) b^2 (1+\rho^2 + 2\rho \cos\varphi)$$

$$+ b^4 \{1+4\rho^2 + \rho^4 + 4\rho(1+\rho^2) \cos\varphi + 2\rho^2 \cos 2\varphi\}]$$

By equation (115), the complete stress function $\Phi(\rho,\varphi)$ is the sum of equations (136), (137), and (138). The stress components in terms of $\Phi(\rho,\varphi)$ are

$$\left.\begin{array}{l} \sigma_\rho = \dfrac{1}{\rho}\dfrac{\partial\Phi}{\partial\rho} + \dfrac{1}{\rho^2}\dfrac{\partial^2\Phi}{\partial\varphi^2} \\[2em] \sigma_\varphi = \dfrac{\partial^2\Phi}{\partial\rho^2} \\[2em] \tau_{\rho\varphi} = \dfrac{1}{\rho}\dfrac{\partial\Phi}{\partial\varphi} - \dfrac{1}{\rho}\dfrac{\partial^2\Phi}{\partial\rho\,\partial\varphi} \end{array}\right\} \quad (139)$$

From this point on, the algebra is found to be extremely involved. When the boundary conditions are applied to the noncentral holes, namely

$$\left.\begin{array}{l} \sigma_\rho \text{ at } \rho=\lambda = 0 \\[1em] \tau_{\rho\varphi} \text{ at } \rho=\lambda = 0 \end{array}\right\} \quad (140)$$

and the relations of A_n, B_n, A_n', and B_n' in terms of M_{1n}, M_{2n}, M_{3n}, and M_{4n} (equations (111), (112), (113), and (114)) and hence in terms of C_{1s} and C_{3s} (equations (99), (100), (101), and (102)) are recalled, one obtains a set of simultaneous equations involving C_{1s} and C_{3s} only. A formal solution of these equations and equation (110) may be written as

$$C_{1s} = \sum_{t=0}^{\infty} c_{1s}^{(t)}, \qquad C_{3s} = \sum_{t=0}^{\infty} c_{3s}^{(t)} \quad (141)$$

and the feasibility of obtaining the solution depends, in fact, on the convergence of these two series. Once the constants are evaluated, the

stress functions $\Phi(r,\theta)$ and $\Phi(\rho,\varphi)$ are completely determined and, hence, the stresses in the disk.

The analysis assumes the following restrictions to be imposed. $\lambda \left(= \dfrac{c}{b}\right)$ should be chosen in such a way that

$$\left. \begin{aligned} \frac{c}{b-d} &< \sin \frac{\pi}{k} \quad \text{for} \quad \frac{b-d}{a-d} < \frac{1}{1 + \sin \frac{\pi}{k}} \\[3em] \frac{c}{b-d} &< \frac{a-d}{b-d} - 1 \quad \text{for} \quad \frac{b-d}{a-d} \geqq \frac{1}{1 + \sin \frac{\pi}{k}} \end{aligned} \right\} \qquad (142)$$

in order to prevent the boundaries of the holes and the disk from overlapping. Under these conditions, convergence of the series, equation (141), is expected.

CHAPTER IX

RECOMMENDATIONS FOR FURTHER INVESTIGATION

There are many aspects of the problem of centrifugal stresses in rotating disks with central and noncentral holes which remain to be investigated. The analysis of these stresses in a uniform rotating disk with central and noncentral holes presented in Chapter VIII is not complete. A closed form mathematical solution was not obtained because of the complicated nature of the algebra. It is felt that further work in this direction is necessary.

More exhaustive theoretical and experimental analyses are needed in the light of the method of analysis reported in this thesis to investigate the effects of (1) degree of taper, particularly larger taper, (2) the location and (3) the size of the holes on the stress field in the rotating disk by varying one of these parameters at a time keeping the other two constant.

An independent mathematical analysis and solution for elastic stresses in a tapered disk with central and noncentral holes in a centrifugal field is still needed. It is therefore essential to direct attention to this elastic stress problem.

APPENDIX

EXTRAPOLATION OF FRINGE ORDERS AT THE

BOUNDARIES OF NONCENTRAL HOLES

The fringe orders at the edge of the noncentral holes are often hard to read accurately from the photograph of the fringe pattern. This is due to two reasons: first, the fringes occur too closely spaced at the edge of the hole to count them separately, and second, they often occur in their fractional values which are difficult to ascertain exactly.

For an accurate determination of the order of the fringes at the boundary of a noncentral hole, an extrapolation scheme is required. A graphical extrapolation is used in the present work for that purpose.

At a little distance away from the immediate vicinity of the boundary of the hole, the orders of the fringes are easily determined as the fringes appear more distinct and separate from one another. These values of the fringes, n, are plotted against their radial distance, ρ, from the center of the noncentral hole for a constant angle, φ. The curve thus obtained is extended to the edge of the hole. The point of intersection then gives the value of the fringe order at the edge of the hole for that φ as read from the ordinate scale (scale of n).

A set of such graphs for different noncentral holes employed in the investigation is given in Figures 14, 15, and 16.
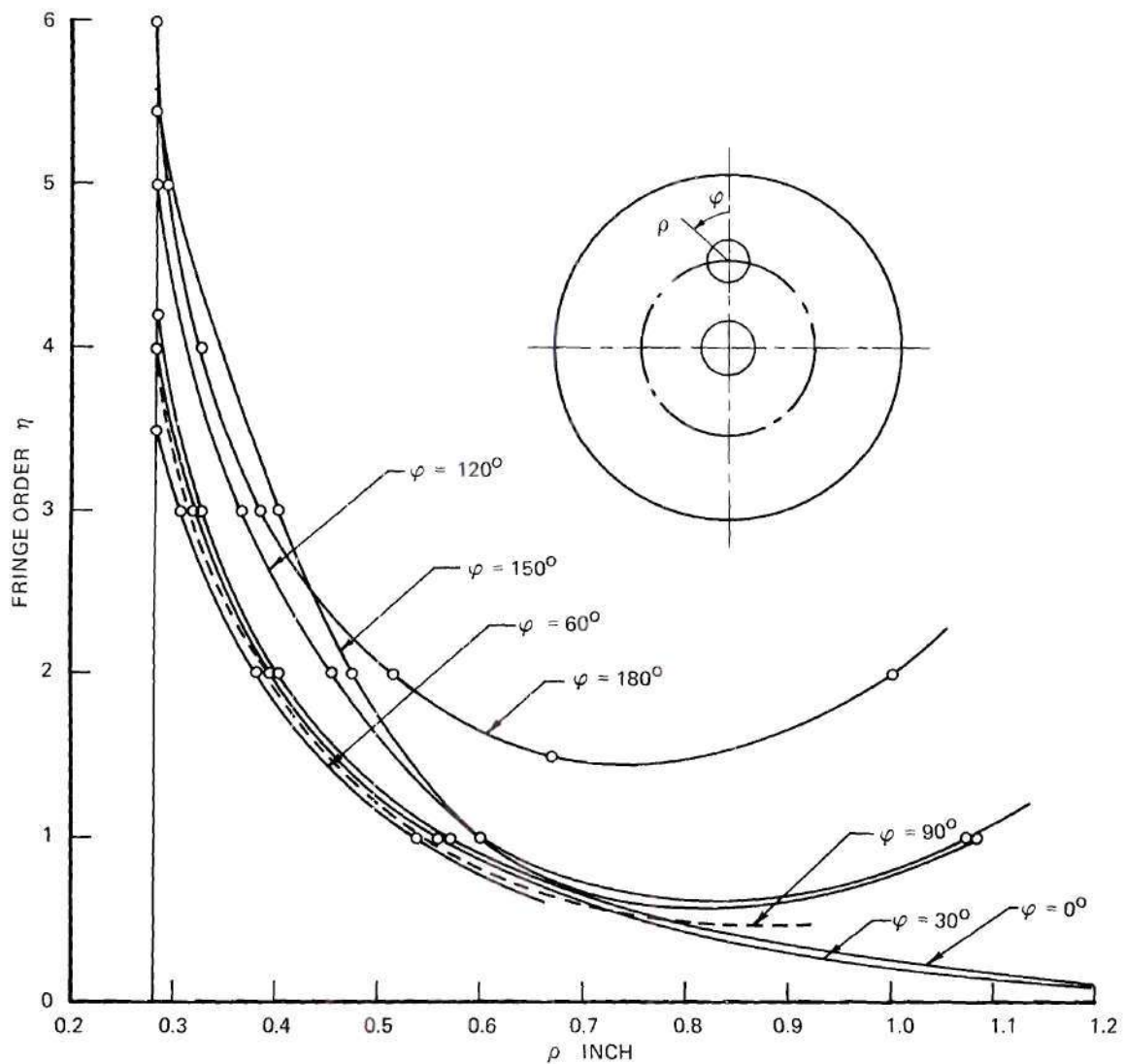
Figure 14.   Auxiliary Graph for Fringe Orders Around 9/16 Inch
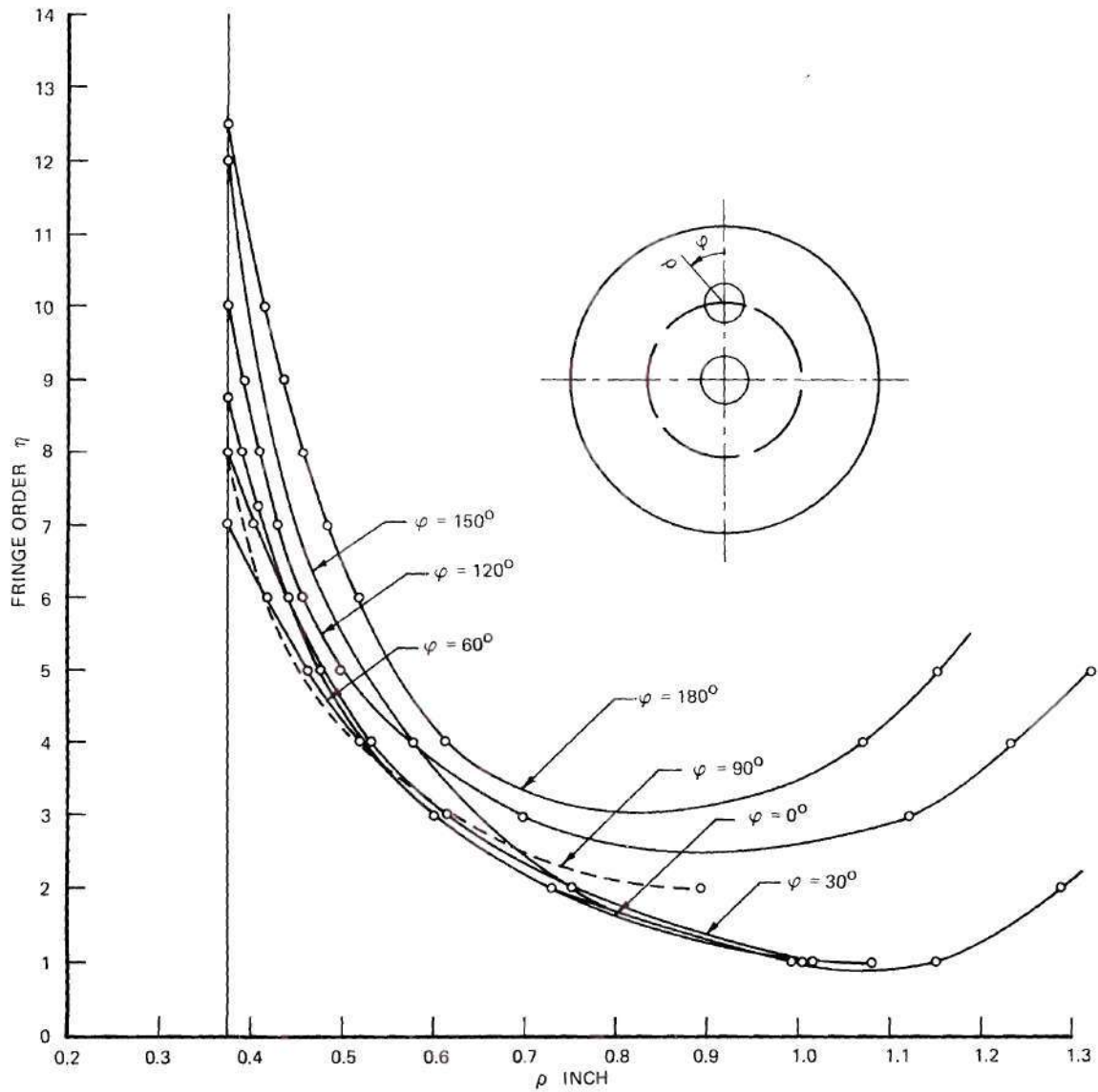Diameter Noncentral Holes

Figure 15. Auxiliary Graph for Fringe Orders Around 3/4 Inch
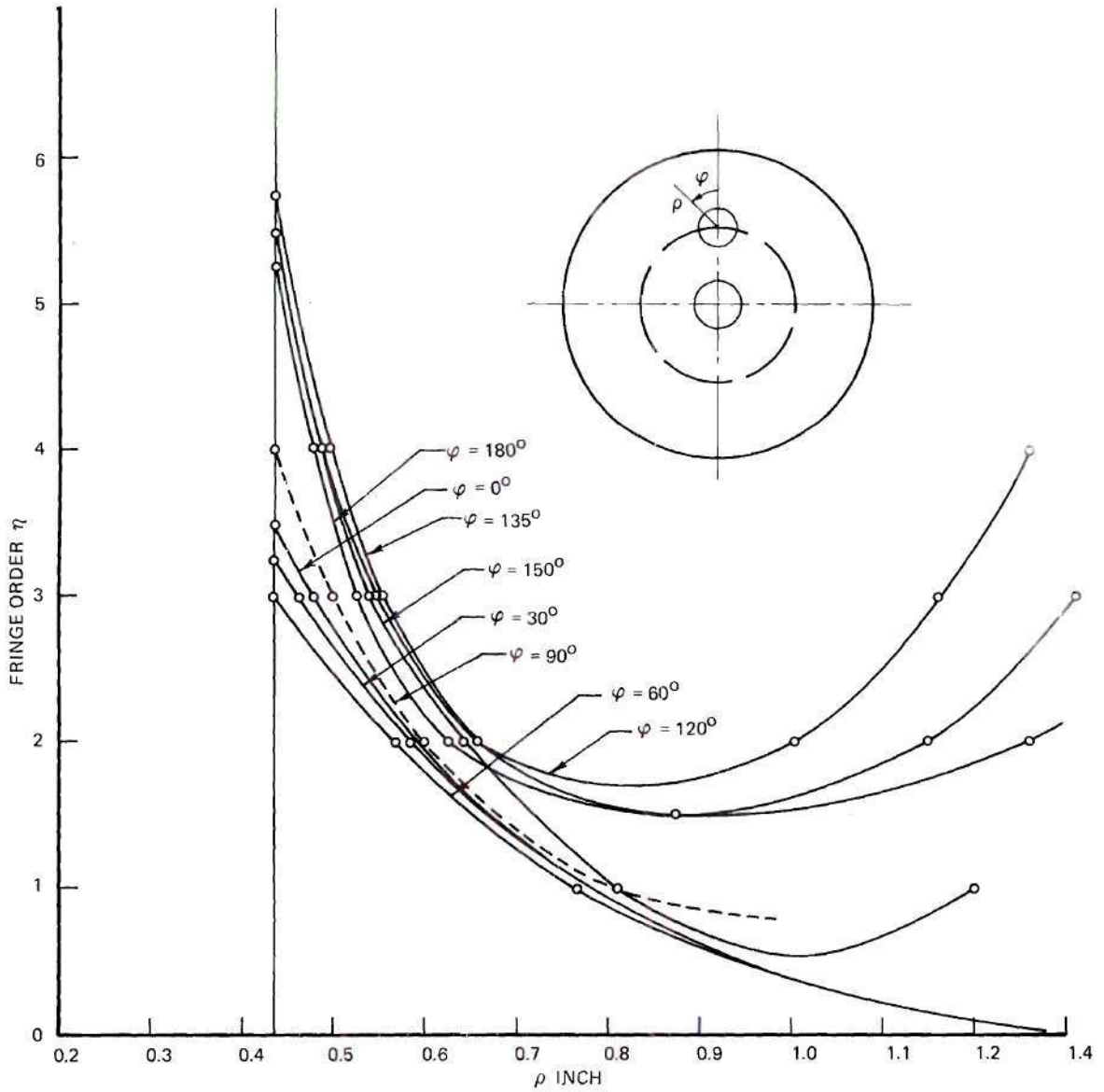Diameter Noncentral Holes

Figure 16. Auxiliary Graph for Fringe Orders Around 7/8 Inch Diameter Noncentral Holes

LITERATURE CITED

1. Armstrong, James H. Stress in rotating tapered disks with noncentral holes. Ph.D. thesis, Iowa State University of Science and Technology, Ames, Iowa, 1960.

2. Armstrong, James H. An investigation of the performance of a modified Tesla turbine. M.S. thesis, Georgia Institute of Technology, Atlanta, Georgia, 1952.

3. Bachlig, E. S. and Conway, H. D. Asymmetrical bending of a cylindrically aelotropic tapered disk. Journal of Applied Mechanics, p. 11, March, 1956.

4. Barnhart, K. E., Jr., Hale, A. L. and Meriam, J. L. Stresses in rotating disks due to noncentral holes. Society for Experimental Stress Analysis Proceedings 9, No. 1 : 35-52, 1951.

5. Bert, C. W. and Niedenfuhr, F. W. Stretching of a polar-orthotropic disk of varying thickness under arbitrary body forces. American Institute of Aeronautics and Astronautics Journal, vol. 1, No. 6, p. 1385, June 1963.

6. Bisshopp, K. E. Stress coefficients for rotating disks of conical profile. Journal of Applied Mechanics 66 : A1-A9, 1944.

7. Chree, C. The stresses and strains in isotropic elastic solid ellipsoids in equilibrium under bodily forces derivable from a potential of the second degree. Proceedings of the Royal Society of London, Series A, 58 : 39-59, 1895.

8. Conway, H. D. Analysis of plane stress in polar co-ordinates and with varying thickness. Journal of Applied Mechanics 26, Transaction American Society of Mechanical Engineers, 81 E, 437-439, 1959.

9. Donath, M. Die Berechnung rotierender Scheiben und Ringe. Berlin, Julius Springer, 1912. Cited in Dinglers Polytechnisches Journal 338 : 217, 1923.

10. Forsyth, A. R. Theory of functions of a complex variable. Third Edition, Dover Publication.

11. Frocht, M. M. Photoelasticity. Vol. 1, New York, John Wiley & Sons, Inc., 1941.

LITERATURE CITED (Continued)

12. Grammel, R. Ein neues Verfahren zur Berechnung rotierender Scheiben. Dinglers Polytechnisches Journal 338 : 217-219, 1923.

13. Green, W. A., Hooper, G. T. J., and Hetherington, R. Stress distribution in rotating disks with noncentral holes. The Aeronautical quarterly, vol. XV, p. 107, May 1964.

14. Hete'nyi, M. Handbook of experimental stress analysis. John Wiley and Sons, Inc., New York, Sixth printing, Sept. 1966.

15. Hodge, P. G., Jr. and Papa, J. Rotating disks with no plane of symmetry. Journal of Franklin Institute. vol. 263, n 6, June 1957, p. 505-22.

16. Honegger. Engineering Dynamics by Biezeno and Grammel, p. 22. Blackie and Sons Ltd. London and Glassgow (1954).

17. Howland, R. C. J. Stresses in a plate containing an infinite row of holes. Proceedings Royal Society of London. A 148, p. 471, 1935.

18. Howland, R. C. J. Potential functions with periodicity in one co-ordinate. Cambridge Philosophical Society Proceedings 29-30, Oct.-Sept. 1932-34.

19. Hulbert, L. E. The numerical solution of two-dimensional problems of the theory of elasticity. Bulletin 198 Engineering Experiment Station, Ohio State University, Columbus, Ohio.

20. Jeffery, G. B. Plane stress and plane strain in bipolar co-ordinates. Philosophical Transactions, Series A, vol. 221, p. 265-293, 1920.

21. Kumar, S. and Jogarao, C. V. Investigation of stresses around a hole in thin rotating disks of hyperbolic and parabolic profiles. Journal of Indian Institute of Science, Bangalore, India. Section B, 35 : 93-102, 1953.

22. Langhaar, H. L. An invariant membrane stress function for shells. Journal of Applied mechanics. vol. 20, p. 178, June 1953.

23. Lee, T. C. On the stresses in a rotating disk of variable thickness. Journal of Applied mechanics 52 : 263-266, 1952.

24. Ling, C. B. and Wang, P. S. Stresses in a perforated plate containing a ring of circular holes. Technical Report no. 6, Chinese Bureau of Aeronautical Research, June 1943.

LITERATURE CITED (Continued)

25. Martin, H. M. Stress distribution in rotating disks of conical profile. Engineering 115 : 1-3, 115-116, 407, 630, 1923.

26. Mindlin, R. D. Stresses in an eccentrically rotating disk. London, Edinborough and Dublin Philosophical megazine. Series 7, 26 : 713-719, 1938.

27. Muskhelishvili, N. I. Some Basic Problems of the mathematical theory of elasticity. Fourth, corrected and augmented edition, Moscow 1954. Translated from Russian by J. R. M. Radok. P. Noordhoff Ltd. Groningen - The Netherlands, 1963.

28. Newton, R. E. A photoelastic study of stresses in rotating disks. Journal of Applied Mechanics 62 : A57-A60, 1940.

29. Saito, H. On the stresses in statical and rotating circular plates having symmetrically placed eccentric holes. Transactions Japan Society of Mechanical Engineers 20(7) 95 : 473-478, 1954.

30. Saito, H. Stresses in rotating circular disks with noncentral circular holes. Technology reports, Tokoku University, vol. 21, No. 2, p. 217, 1957.

31. Saito, H. and Honma, Y. Stresses in rotating tapered disks with noncentral circular holes. Technology Reports, Tohoku University, vol. 30, No. 1, p. 25, 1965.

32. Samanta, B. K. Note on nonhomogeneous rotating circular disks. Indian Journal of Theoretical Physics 12, 2, 41-48, June 1964.

33. Sen, B. Boundary value problems of circular disks under body forces. Bulletin Calcutta Mathematical Society 36, 58-62, 83-86, 1944.

34. Sengupta, A. M. Stresses in some aelotropic and isotropic circular disks of varying thickness rotating about the central axis. Bulletin Calcutta Mathematical Society 41, 129-139, 1949.

35. Stern, M. Rotationally symmetric plane stress distribution. Zeitschrift für Angewandte Mathmatik und Mechanik 45,6, 446-447, Nov. 1965.

36. Stodola, A. Dumpf und Gas Turbinen. Authorized translation to the second edition by Dr. Lewis C. Loewenstein, New York, D. Van Nostrand Co., 1905.

37. Timoshenko, S. Theory of Elastocity. 2nd edition, New York, McGraw-Hill Book Company, Inc., 1951.

LITERATURE CITED (Concluded)

38.   Udoguchi, T. Analysis of centrifugal stresses in a rotating disk
containing an eccentric circular hole. Japan Science Review,
Series 1, 1, No. 1 : 55-63, 1949.

VITA

Amrit Kumar Paul was born in Baripada, Orissa, India on April 2, 1937. He attended the elementary schools, the high schools, and two years of College education in Intermediate of Science there. He secured the fifth rank in the final high school examinations (1953) and the eighth rank in the final I.Sc. examinations (1955) conducted by the Utkal University, the only university in the State of Orissa at that time, and received merit scholarships.

From 1955 to 1959 he attended the College of Engineering and Technology, Jadavpur University, Calcutta, where he received the degree of Bachelor of Mechanical Engineering with honors, securing the third rank in the University.

He then taught as a lecturer in the Department of Mechanical Engineering at the University College of Engineering, Burla, Orissa until June 1964. During 1962-1963 he took study leave for a year and attended the Indian Institute of Technology, Kharagpur. He received the degree of Master of Technology in Machine Design (Mechanical) from this institute. In June 1964, he joined the Department of Mechanical Engineering at Regional Engineering College, Rourkela, Orissa as Assistant Professor.

He came to the Georgia Institute of Technology in Fall, 1966.

He was married to Shakuntala on April 24, 1960. The couple has a daughter and a son.